

1 **Title:**

2 **Salmonella injectisome penetration of macrophages triggers rapid translation of**  
3 **transcription factors and protection against cell death**

4

5 **Short title:**

6 **Salmonella injectisome interaction triggers rapid host translational induction**

7

8 **Authors**

9 George Wood<sup>a, §</sup>, Rebecca Johnson<sup>a, §</sup>, Jessica Powell<sup>a</sup>, Owain J. Bryant<sup>a</sup>, Filip Lastovka<sup>a</sup>,  
10 Matt Brember<sup>a</sup>, Pani Tourlomousis<sup>b</sup>, John P. Carr<sup>c</sup>, Clare E. Bryant<sup>b\*</sup> and Betty Y.W. Chung<sup>a,\*</sup>

11

12 **Affiliations**

13 <sup>a</sup> Department of Pathology, University of Cambridge, Tennis Court Road, Cambridge, CB2  
14 1QP, United Kingdom

15 <sup>b</sup> Department of Medicine and Department of Veterinary Medicine, University of Cambridge,  
16 Madingley Rd, Cambridge CB3 0ES, United Kingdom

17 <sup>c</sup> Department of Plant Sciences, University of Cambridge, Downing Street, Cambridge CB2  
18 3EA, United Kingdom

19

20 <sup>§</sup> These authors contributed equally

21

22 **Corresponding authors:** [ceb27@cam.ac.uk](mailto:ceb27@cam.ac.uk), [bcy23@cam.ac.uk](mailto:bcy23@cam.ac.uk)

23

24 *'For the purpose of open access, the author has applied a Creative Commons Attribution*  
25 *(CC BY) licence to any Author Accepted Manuscript version arising'*

26

27 **Abstract**

28 During bacterial infection both the host cell and its invader must divert intracellular resources  
29 to synthesise specific proteins in a timely manner. For the host, these factors may be needed  
30 for innate immune responses, including programmed cell death, and in the bacteria newly  
31 synthesized proteins may be survival factors needed to counteract host responses.  
32 *Salmonella* is an important food-borne bacterial pathogen that invades and multiplies within  
33 host cells. It is well established that invasion of epithelial cells is dependent upon the SPI-1  
34 Type III injectisome, a biological needle that penetrates and secretes effectors into host cells  
35 to promote internalization. However, the importance of the SPI-1 injectisome in infection of  
36 professional phagocytes such as macrophages, which are the predominant host cell type

37 during systemic infection, is less clear. Through time resolved parallel transcriptomic and  
38 translatomic studies of macrophage infection, we revealed that SPI-1 injectisome-dependent  
39 infection of macrophages triggers rapid translation of transcription factor mRNAs, including  
40 Early Growth Response 1 (*Egr1*). Despite the short half-life of EGR1 protein, its swift synthesis  
41 within the initial hour of infection is sufficient to inhibit transcription of pro-inflammatory genes  
42 and thereby restrain inflammatory responses and programmed cell death within the first hour  
43 of during early infection. This transient period of inflammatory suppression in macrophages is  
44 exploited by *Salmonella* to establish infection and sheds new insight on the importance of  
45 translational activation in host-pathogen dynamics during *Salmonella* infection.

46 **Introduction**

47 The gene expression profiles of both host<sup>1–5</sup> and pathogen<sup>6</sup> are altered dramatically when  
48 they interact. This response is shaped by a co-evolutionary arms race where the host seeks  
49 to detect and counter the invading pathogen<sup>3,5</sup>, whilst the pathogen aims to evade this  
50 response<sup>6</sup> and modify the host environment to better suit its survival and replication<sup>1,2</sup>.  
51 Changes in gene expression during infection are thus the net result of these competing  
52 goals, the balance of which can ultimately determine the infection outcome.

53

54 Many members of the Gram-negative bacterial genus *Salmonella* are facultative intracellular  
55 pathogens that infect a diverse spectrum of hosts. *Salmonella* species cause a range of  
56 diseases in humans, from typhoid fever to gastroenteritis. *Salmonella*'s ability to establish an  
57 intracellular infection is key to its pathogenesis<sup>7</sup>. During infection, the bacterium invades host  
58 cells, including the epithelial cells lining the intestinal tract and immune cells such as  
59 macrophages. Once internalized, *Salmonella* resides in a specialised membrane-bound  
60 compartment, the *Salmonella*-containing vacuole (SCV). The SCV provides a protective  
61 niche for the pathogen while giving it access to host cell nutrients to support its replication<sup>8,9</sup>.

62

63 The intracellular lifestyle of pathogenic *Salmonella* is supported by two Type III secretion  
64 systems (T3SS) with different substrate specificity. The SPI-1 T3SS, also called the SPI-1  
65 injectisome (hereafter, 'injectisome') is a multi-protein complex that spans the bacterial inner  
66 and outer membranes and cell wall, and transports proteins into target cells along a  
67 homomeric needle-like structure that is inserted into the host cell membrane by the bacterial  
68 effectors SipB, SipC and SipD<sup>10–12</sup>. PrgJ forms the inner rod that connects the injectisome  
69 basal body embedded in the *Salmonella* envelope with the needle structure and thus acts as  
70 a channel bridging the bacterial and host cytoplasms<sup>10</sup>. In epithelial cells, the injectisome is  
71 important in aiding host cell invasion via the trigger mechanism<sup>13–15</sup>, though its role in  
72 establishing infection in professional phagocytes, such as macrophages, is less well

73 understood. The SPI-2 T3SS is expressed once the bacterium is internalized and supports  
74 the intracellular lifecycle of the pathogen<sup>8,16</sup>.

75

76 To allow transport of effector proteins via the injectisome into the host cell, the *Salmonella*  
77 translocon subunits SipB and SipC are also secreted via the injectisome and inserted into  
78 the host cell plasma membrane to form a transient pore<sup>11,12,17,18</sup>. This insertion leads to  
79 transient loss of membrane integrity, therefore triggering an osmotic stress response and  
80 collapse of ion gradients with Ca<sup>2+</sup> influx, and Cl<sup>-</sup> and K<sup>+</sup> efflux. Injectisome-dependent  
81 membrane damage is demonstrated by the haemolysin activity of the injectisome on red  
82 blood cells, which lyse upon SipBC insertion into their membranes<sup>12</sup>. While it is known that  
83 loss of membrane integrity, and the associated disruption of ion gradients, triggers  
84 inflammatory response pathways and cell death<sup>17,19,20</sup>, the importance of this damage in  
85 eliciting host responses to *Salmonella* remains unclear.

86

87 In systemic infection, macrophages are the predominant host cell type and *Salmonella*  
88 survival in macrophages has been reported to be critical for virulence<sup>7,21</sup>. This is somewhat  
89 paradoxical given the importance of macrophages for the detection and elimination of  
90 pathogens<sup>22</sup>. Indeed, macrophages possess many receptors that detect *Salmonella* pathogen  
91 associated molecular patterns (PAMPs), which are crucial in controlling infection. This  
92 includes toll-like receptors (TLRs) such as TLR4 which detects bacterial lipopolysaccharide  
93 (LPS) on the *Salmonella* cell surface<sup>23</sup> as well as intracellular immune receptors that can  
94 activate the inflammasome and lead to inflammatory cell death<sup>24–26</sup>. In tissue culture, the  
95 majority macrophages die within the first few hours of infection<sup>27–29</sup> and this rapid cytotoxicity  
96 is dependent on the injectisome<sup>27,29</sup>. The balance between macrophage survival and death  
97 will influence the outcome of infection<sup>22</sup>.

98

99 Although much research has been carried out on the transcriptional response of host cells to  
100 *Salmonella* infection<sup>2–4</sup>, the analysis of gene expression is incomplete without also exploring  
101 regulation at the level of translation, i.e. protein synthesis. This is of particular importance  
102 given the critical nature of events occurring very early in infection. Translational regulation  
103 has the potential to allow for rapid responses, either through modulating translation of pre-  
104 existing mRNAs and/or by enhancing translation of the newly transcribed mRNAs. Indeed,  
105 previous studies have identified potent translational upregulation of inflammatory genes,  
106 such as *Tnf*, in macrophages following stimulation of TLR4 with purified LPS<sup>30,31</sup>.

107

108 Here we utilized paired ribosome profiling and RNA-Seq over a time course of infection with  
109 wild type or SPI-1 injectisome mutant *Salmonella* in macrophages to understand the

110 dynamics of gene expression regulation throughout injectisome-dependent infection. We  
111 identified that the translational response precedes the transcriptional response within sixty  
112 min post infection, and it is enriched for genes that encode DNA binding proteins. Within the  
113 translationally induced DNA binding proteins, we identified Early Growth Response 1 (*Egr1*).  
114 *Egr1* showed rapid injectisome-dependent transcriptional induction, with even greater  
115 translational induction, enabling the rapid and robust production of the EGR1 transcription  
116 factor early in infection. We further demonstrated that, while the EGR1 protein turnover is  
117 rapid, it acts as a longer term transcriptional suppressor of inflammatory genes triggered by  
118 *Salmonella* infection. We hypothesize that this creates an early window of opportunity for  
119 *Salmonella* to circumvent innate immunity, allowing it to successfully establish infection.

120

## 121 **Results**

### 122 ***Salmonella* infection triggers rapid host cell responses**

123 *Salmonella* entry into immortalized murine bone marrow derived macrophages (iBMDM,  
124 hereafter ‘macrophages’ unless otherwise stated) is markedly enhanced by the injectisome,  
125 although the mechanism in which it is involved in the invasion of professional phagocytes is  
126 unclear<sup>13–15,32</sup>. *Salmonella* cells associated with host cell membrane, i.e. actively invading  
127 bacteria, were seen as early as 5 min post-exposure, with *Salmonella* rapidly internalized  
128 within 15 min (Figure 1A-B). There was little further macrophage infection after 15 min of  
129 infection, indicating a potential change in susceptibility (Figure S1A). Injectisome-  
130 independent internalization was assayed through infection with mutant *Salmonella* unable to  
131 assemble the injectisome needle, generated by knockout of the SPI-1 inner-rod protein  
132 PrgJ<sup>33</sup> and referred to as the ‘injectisome mutant’ hereafter. Invasion by injectisome mutant  
133 *Salmonella* was also observable within this timeframe, though to a lesser degree than for  
134 wildtype (WT) bacteria (Figure S1B).

135

136 As previously described<sup>27–29</sup>, infection of macrophages with WT *Salmonella* led to rapid cell  
137 death within the first 60 min of infection. However, approximately 25% of macrophages  
138 survived despite the presence of viable intracellular bacteria (Figure 1C-D, S1A). In contrast,  
139 and similar to previous studies<sup>34</sup>, infection with injectisome mutant *Salmonella* did not induce  
140 any increase in macrophage cell death (Figure 1D).

141

### 142 **Injectisome-dependent infection leads to both transcriptional and translational 143 induction of Early Growth Response 1 (EGR1) accumulation**

144 As a significant proportion of macrophages survive the lethal effect of injectisome  
145 penetration (Figure 1A-D), we hypothesized that survival of infected cells beyond 60 min  
146 post-infection with WT *Salmonella* may be a consequence of rapid gene expression

147 responses occurring within the first hour. This may be mediated by *de novo* transcription of  
148 mRNAs, which has been the focus for most previous studies<sup>2-4</sup>. However, we suspected the  
149 involvement of translational responses, which remain much less well understood, where the  
150 rate of protein synthesis (translational efficiency) from mRNAs may be upregulated to  
151 increase protein abundance more rapidly than could occur *via* transcription alone. Such an  
152 acceleration of protein synthesis could be of critical importance given the short survival  
153 timeframe of most infected cells. To investigate rapid transcriptional and translational  
154 changes in gene expression, parallel global transcriptomic (RNA-Seq) and translatomic (i.e.,  
155 ribosome profiling, Ribo-Seq hereafter) analyses were performed on macrophages at 60 min  
156 following infection with either WT *Salmonella* or the injectisome mutant (Figure 1E, S1C).  
157 Ribo-Seq is a highly sensitive method that reveals the global translatome at the time of  
158 harvest<sup>35</sup>. The technique determines the position of ribosomes by exploiting the protection  
159 from nuclease digestion of a discrete fragment of mRNA (~30 nucleotides) conferred by  
160 elongating ribosomes. Deep sequencing of these ribosome-protected fragments (RPFs)  
161 generates a high-resolution view of the location and abundance of translating ribosomes on  
162 different mRNA species, reflecting the amount of synthesis of specific proteins (Figure 1E).  
163 In addition, while RNA-Seq enables quantification of total mRNA abundance, parallel RNA-  
164 Seq and Ribo-Seq enables quantification of translation efficiency, a measurement of how  
165 well each mRNA is being translated as distinct from total protein synthesized (Figure 1F).  
166  
167 The resolution of our Ribo-Seq data is high, as evident from the metagene analysis  
168 constructed with the software program riboSeqR<sup>36</sup>. The metagene translatome is a summed  
169 plot of all translated mRNAs, with weighted average number of nucleotide reads around the  
170 annotated coding start and stop sites, confirming accurate capture of the elongating  
171 ribosome movement as almost all Ribo-Seq reads overwhelming maps to the first codon  
172 position (S1C). This is further evidenced by our ability to directly visualize translation of  
173 single genes at remarkable accuracy (Figure 1I), as well as non-canonical translation events.  
174 For example, translation of *Atf4*, which is modulated by translation of two small upstream  
175 open reading frames (uORFs) embedded within the 5'UTR of ATF4<sup>37</sup> (Figure S1E). The high-  
176 resolution nature of our data therefore enables accurate quantification of protein synthesis  
177 (i.e. total Ribo-Seq) and translational efficiency when combined with parallel RNA-Seq  
178 (Figure 1F).  
179  
180 Initial analysis of macrophages infected by both WT and injectisome mutant *Salmonella*  
181 identified many genes known to be upregulated upon exposure to bacterial PAMPs<sup>30,31,38</sup>,  
182 such as *Tnf* and *Zfp36*. These genes were upregulated not only in transcript abundance but  
183 also at the translational level (Figure 1G, H, I and S1D and F). For both of these genes,

184 transcription was induced in response to either the WT or injectisome mutant *Salmonella*.  
185 Potent translational upregulation was also seen, i.e. enhanced translational efficiency  
186 resulting in greater protein synthesis than can be explained by an increase in *de novo* mRNA  
187 synthesis alone (see Figure 1F), as has been previously reported in macrophages exposed  
188 to purified bacterial LPS<sup>30,31</sup>.

189  
190 Following this, transcripts that were subject to specific injectisome-dependent translational  
191 upregulation were investigated (Figure S1F). The key inflammasome component *Nlrp3* was  
192 among the selectively induced genes (Figure S1G). The *Nlrp3* transcript has recently been  
193 described to encode a uORF<sup>39</sup> which can be readily visualised in this data (Figure S1H). The  
194 NLRP3 is activated in *Salmonella* infection but the uORF-mediated translational regulation of  
195 *Nlrp3* is currently unclear<sup>33,40,41</sup>. To further identify injectisome-dependent translationally  
196 regulated genes, transcripts where the log<sub>2</sub> fold-change (log<sub>2</sub>FC) in translational efficiency  
197 was greater than 1.5 in WT *Salmonella* infected macrophages over macrophages infected by  
198 the injectisome mutant were selected (Figure 1J). Amongst the most translationally  
199 upregulated mRNAs were those encoding Early Growth Response 1 (EGR1), NR4A1 and  
200 Pro-Interleukin-1 beta (pro-IL-1 $\beta$ ) (Figure 1J-K).

201  
202 Interleukin-1 beta (IL-1 $\beta$ ) is processed from its precursor pro-IL-1 $\beta$  into its mature, active  
203 form by caspases; proteases that are themselves activated by the inflammasome<sup>26,42</sup>. This  
204 precursor, encoded by *Il1b*, had a much greater translation efficiency in macrophages  
205 infected by WT *Salmonella* than the injectisome mutant (Figure 1J-K). The injectisome is  
206 known to transport bacterial effectors into the host cytosol that activate the inflammasome,  
207 including components of the translocon such as SipB/C<sup>43,44</sup>, consistent with our cytotoxicity  
208 assay (Figure 1D), leading to IL-1 $\beta$  production<sup>25,45</sup>. These data suggest that IL-1 $\beta$  precursor  
209 production is supported not only by increased mRNA transcription, but also post-  
210 transcriptionally by specific upregulation of translation of its mRNA. Previous reports  
211 describe the need for two signals to produce IL-1 $\beta$ : one to induce transcription of the  
212 precursor and another to activate the inflammasome<sup>43,46,47</sup>. Importantly, however, our data  
213 additionally reveal a strong role for translational upregulation in precursor production to  
214 rapidly facilitate overall IL-1 $\beta$  precursor protein production. Therefore, the injectisome makes  
215 an important contribution to macrophage pro-IL-1 $\beta$  production within the first 60 min, in  
216 addition to delivering the factors that stimulate pro-IL-1 $\beta$  cleavage leading to IL-1 $\beta$   
217 production.

218  
219 Both *Egr1* and *Nr4a1* are known immediate early genes that are rapidly transcribed in many  
220 cell types within minutes in response to a range of cellular stresses<sup>48-50</sup>. Here we show that

221 while transcripts for both genes are almost absent in uninfected macrophages, rapid  
222 expression of these genes is enhanced by specific transcriptional upregulation leading to a  
223 surge of translational activation following injectisome-dependent infection (Figure 1J-K).  
224 NR4A1, also known as NUR77, is involved in macrophage responses to proinflammatory  
225 stimuli. NR4A1 limits inflammation in models of sepsis and colitis, likely through antagonism  
226 of the NF- $\kappa$ B pathway<sup>51,52</sup>. More recently, however, it has been reported to increase  
227 expression of proinflammatory cytokines in mice infected with *Klebsiella pneumoniae*<sup>53</sup>. The  
228 role of NR4A1 is therefore certainly immunomodulatory but likely differs by cell type and  
229 context.

230  
231 Of the three transcripts chosen for detailed study, the most translationally induced is the  
232 mRNA for EGR1 (Figure 1J-K). EGR1 is a zinc-finger family transcription factor that binds  
233 GC-rich consensus sequences in gene promoters and enhancers, and it can either activate  
234 or suppress transcription. Targets of EGR1 span diverse biological processes including  
235 immune responses, cell growth and differentiation, and cell death<sup>54–59</sup>. Due to its highly  
236 injectisome-dependent translational upregulation, the biological function of EGR1 in  
237 *Salmonella*-macrophage infection was further characterized in this study.

238  
239 **Specific upregulation of EGR1 protein accumulation during the macrophage-**  
240 ***Salmonella* interaction is highly injectisome-dependent**  
241 Transcriptional upregulation of *Egr1* has previously been shown to be largely dependent on  
242 bacterial secretion systems in other infection contexts<sup>2,60–62</sup>. However, EGR1 has not been  
243 studied in the context of *Salmonella* infection of macrophages nor has post-transcriptional  
244 regulation of *Egr1* gene expression been studied. We were particularly interested in EGR1  
245 given its association with cell death<sup>54</sup> and its importance in macrophage development<sup>49,57</sup>.

246  
247 At 60 min post-infection there was a clear increase in both transcription and translation of  
248 *Egr1* in WT-infected cells (Figure 1K, I and 2A). The increase in *Egr1* translation cannot be  
249 explained by the greater transcript abundance alone, but rather there is also an increase in  
250 *Egr1* mRNA translation efficiency. The translational efficiency of *Egr1* mRNA is three times  
251 higher in WT-infected cells compared to cells infected with the injectisome mutant (Figure  
252 1K, I and 2A). In contrast, the *Egr1* expression in cells infected with the injectisome mutant  
253 were not much greater at 60 min post infection than in mock-infected cells. Reverse  
254 transcription-coupled quantitative PCR (RT-qPCR) for *Egr1* mRNA and immunoblot for  
255 EGR1 protein accumulation showed that during an infection time-course the upregulation  
256 was rapid but transient and that the half-lives of both *Egr1* mRNA and its protein product are  
257 short. While *Egr1* mRNA abundance peaked at 60 min and returned to baseline levels by

258 120 min (Figure 2B and C), the increase in protein abundance measured by immunoblotting  
259 was, as expected, offset from the increase in mRNA, peaking at 120 min post-infection and  
260 returning to undetectable levels by 240 min. The absence of EGR1 protein 240 min post-  
261 infection indicates a short half-life for EGR1 protein and that its biological effect is likely rapid  
262 (Figure 2C-D). In contrast, infection with the injectisome mutant led to a slight increase in  
263 *Egr1* mRNA abundance at 60 min, followed by a detectable increase in EGR1 protein by 120  
264 min, with both mRNA and protein at considerably lower levels than in WT *Salmonella*  
265 infected cells (Figure 2A-D).

266

267 We reasoned that both *Egr1* transcriptional stimulation and the potent translational induction  
268 (i.e. higher translational efficiency) could be either a result of the direct interaction of the  
269 injectisome with macrophage, through insertion of the SipB/C translocon complex into the  
270 macrophage plasmalemma<sup>18</sup>, or due to transport of effector proteins once the injectisome is  
271 fully assembled and is in a secretion competent state. To distinguish between these  
272 possibilities, we engineered an injectisome blocking substrate in which the effector protein  
273 SptP is C-terminally fused to the green fluorescent protein (SptP-GFP). This injectisome  
274 blocking substrate is targeted to the export machinery and stalls within the injectisome  
275 export channel because the folding of the GFP moiety (unlike the effector protein sequence)  
276 is irreversible. Stalling occurs after needle assembly is complete, thereby blocking transport  
277 of effectors and translocon subunits through the injectisomes that have assembled on the  
278 bacterial cell surface<sup>63</sup>, preventing penetration of macrophage plasmalemma (Figure 2E-F).  
279 Obstructing the injectisome enabled us to uncouple the effect on *Egr1* upregulation upon  
280 penetration of macrophage plasmalemma by the injectisome from transport of effector and  
281 translocon subunits.

282

283 Expression of the SptP-GFP injectisome blocking substrate was controlled in the following  
284 manner: (1) uninduced, therefore recapitulates WT infection where the injectisome  
285 penetrates macrophages and delivers effectors; (2) Inducing expression of the blocking  
286 substrate 2 h prior to macrophage infection, resulting in assembly of injectisomes that are  
287 blocked with the SptP-GFP blocking substrate, preventing delivery of effectors whilst at the  
288 same time preventing delivery and insertion of translocon subunits (SipB/SipC) into the host  
289 cell membrane, which consequently abolishes penetration of macrophage plasmalemma;  
290 and (3) blockage of injectisome induced at 5 min post-infection, therefore allowing  
291 injectisomes to penetrate macrophage plasmalemma while inhibiting further delivery of  
292 effectors (Figure 2E). As expected, transcription of *Egr1* was upregulated when  
293 macrophages were infected by *Salmonella* with unobstructed injectisome (uninduced), but  
294 expression is significantly impaired in macrophages challenged by *Salmonella* with a pre-

295 blocked, translocon-defective injectisome. However, *Egr1* transcript accumulation was only  
296 slightly reduced when penetration of injectisome is established but delivery of effector is  
297 prevented by SptP-GFP induction at 5 min post-infection (Figure 2G). Taken together, these  
298 results suggest that the trigger for overall *Egr1* protein accumulation occurs very rapidly  
299 during infection and is likely a direct result of injectisome penetration with the macrophage  
300 plasmalemma or the action of the first few effector molecules that make it through the  
301 injectisome.

302

303 **EGR1 protein restrains macrophage inflammatory responses to *Salmonella* infection**

304 To further investigate the role of EGR1 during injectisome dependent infection of  
305 macrophages, we generated EGR1 knockout ( $EGR1^{KO}$ ) macrophages using CRISPR-Cas9  
306 and confirmed the absence of EGR1 protein 120 min after infection with WT *Salmonella*  
307 (Figure 2H). Mutation of the *Egr1* coding sequence resulting in EGR1 knock-out in  $EGR1^{KO}$   
308 macrophages was confirmed through genomic DNA sequencing (Figure S2A). Loss of the  
309 ability to produce EGR1 resulted in greater cell death at baseline, and this was further  
310 increased when infected by WT *Salmonella*, particularly between 30 and 120 min post  
311 infection (Figure 2I). This suggests EGR1 may play a role in limiting injectisome-induced  
312 macrophage death. Following this, the role of EGR1 in the inflammatory response was  
313 assessed by measuring the level of IL-1 $\beta$  produced by  $EGR1^{KO}$  and  $EGR1^{WT}$  macrophages  
314 during infection. This revealed significantly greater upregulation in  $EGR1^{KO}$  macrophages  
315 infected with WT *Salmonella*, confirming that EGR1 has a suppressive role in the  
316 inflammatory response.

317

318 As EGR1 is annotated as a DNA-binding protein, we hypothesized that EGR1 suppresses  
319 inflammation through transcriptional regulation and so time-resolved transcriptomic analysis  
320 (RNA-Seq) of WT *Salmonella*-infected  $EGR1^{KO}$  or  $EGR1^{WT}$  macrophages from 15 to 240 min  
321 post infection was performed. Principal component analysis of gene transcript levels showed  
322 a clear separation of samples by cell line and time post-infection. Principal component (PC)  
323 1 largely reflects variation between the  $EGR1^{KO}$  and  $EGR1^{WT}$  cell lines, whereas PC2  
324 separates the 120 min and 240 min infected samples from the 15 to 60 min infected samples  
325 and 15 to 240 min mock inoculation treatments (Figure S2B). We observed a significant  
326 increase in the abundance of transcripts associated with immune responses in the  $EGR1^{KO}$   
327 macrophages compared to the  $EGR1^{WT}$  macrophages, particularly at 240 min post-infection,  
328 confirming the suppression of transcription of inflammatory genes by EGR1 during  
329 *Salmonella* infection (Figure 2K-L; Table S1-2). This includes *Il1b*, which showed greater  
330 upregulation of transcription in  $EGR1^{KO}$  macrophages infected with WT *Salmonella*. This is  
331 likely the cause of the greater IL-1 $\beta$  secretion during *Salmonella* infection in the absence of

332 EGR1 (Figure 2J) and confirmed EGR1 as an important transcriptional immunomodulator. In  
333 addition, gene ontology enrichment analysis also revealed significant upregulation of known  
334 pro-cell death genes in infection of the EGR1<sup>KO</sup> macrophages, including the FAS death  
335 receptor, consistent with a role of EGR1 in limiting macrophage death (Figure 2L; Table S1-  
336 2).

337

338 **The transcriptional and translational dynamics of *Salmonella* during macrophage  
339 infection**

340 We have demonstrated that injectisome-dependent infection triggers surges both in *de novo*  
341 mRNA synthesis and in translational efficiency of specific host mRNAs such as *Egr1*, leading  
342 to rapid but transient accumulation of EGR1 protein. To assess global expression dynamics  
343 throughout *Salmonella* infection, we therefore performed time-resolved parallel RNA-Seq  
344 and Ribo-Seq of primary bone marrow-derived macrophages infected with WT *Salmonella* or  
345 the injectisome mutant (Figure 3A). The use of primary macrophages (rather than the  
346 iBMDMs used in previous experiments) allows us to compare injectisome- *versus* PAMP-  
347 dependent responses in a system that more closely resembles *in vivo* infection. The primary  
348 macrophages showed similar rates of infection to iBMDMs for WT *Salmonella*, but a greater  
349 proportion were infected with the injectisome mutant compared to iBMDMs (Figure S1B and  
350 S3A).

351

352 Due to the nature of the mRNA enrichment and library preparation method employed, both  
353 host and bacterial translational and transcriptional dynamics were simultaneously captured  
354 over the course of infection. Transcription and translation were also assessed in *Salmonella*  
355 grown in Luria Broth (or lysogeny broth, LB) at various optical densities (OD). It has been  
356 established that expression of SPI-1 in LB culture peaks at late exponential phase, OD 2<sup>29</sup>,  
357 as they were prepared for in these infection assays. This data demonstrates this increase in  
358 expression of SPI-1 injectisome structural genes as the bacteria approach OD 2, through  
359 enhanced translation (Figure 3B). Remarkably, we see significant transcriptional induction of  
360 SPI-1 genes upon contact with macrophages, particularly structural components such as Prg  
361 I/J and K, as early as 5-15 min. aligning with the timeframe of the initial *Salmonella*-  
362 macrophage interaction (Figure 1A-C). This indicates that *Salmonella* respond to the  
363 proximity of macrophages by upregulating expression of certain genes that enable invasion  
364 (Figure 3B), and suggests that rapid assembly of injectisomes occurs on the bacterial cell  
365 surface during the first 15 min. Indeed, the rapid assembly of additional T3SSs upon contact  
366 with host cells has also been suggested in *Yersinia enterocolitica* infection<sup>64</sup>. The  
367 transcriptional and translational response of non-structural SPI-1 genes that encode effector  
368 proteins, structural genes with a dual-role as effectors such as *SipB* and *SipC*, and other

369 virulence factors also increased during the first 15 min whereas some genes, such as for  
370 *AvrA* and *lacP*, were maximally expressed between 2-4 h post infection (Figure 3B).

371

372 Notably, during the early stages of infection (within the first 30 min), we also observed  
373 increases in the translation efficiency of a subset of intramacrophage genes, including *htrA*,  
374 *hisG* and *cpxP* (Figure 3B). Intramacrophage genes play a crucial role in the survival and  
375 replication of the bacterium inside macrophages and in general maximal transcription for  
376 these genes occurs later. The functions of these genes include roles in magnesium and  
377 phosphate transport and the envelope stress response<sup>65,66</sup>. At the 30 min and 60 min time  
378 points, when *Salmonella* is intracellular and after SCV acidification<sup>67</sup>, the transcript  
379 abundance of SPI-2 genes increases while the abundance of the majority of SPI-1  
380 transcripts decreases (Figure 3B). This agrees with the recognized switch of *Salmonella*  
381 secretion mediated by the transcriptional regulator SsrB. Concurrently we observed  
382 decreases in expression of the flagella components, consistent with previously reported  
383 SsrB-mediated repression<sup>65,68,69</sup> (Figure 3B).

384

385 **A global translational response precedes transcriptional responses in macrophages  
386 following injectisome penetration.**

387 Analysis of parallel Ribo-Seq and RNA-Seq throughout the infection time course provided a  
388 global perspective of the dynamics of host gene expression at multiple levels, notably  
389 changes in RNA abundance and translation efficiency, by comparing primary macrophages  
390 infected with either WT *Salmonella* or the injectisome mutant with mock infection (Figure  
391 S4A). Within 5 min post infection, we can readily visualize that both WT and injectisome  
392 mutant *Salmonella* induced rapid changes in translation efficiency of many genes compared  
393 to mock, with more genes that are translationally induced in an injectisome-dependent  
394 manner (Figure S4B). Furthermore, comparison of WT *Salmonella* and injectisome mutant  
395 infections revealed that injectisome-specific translational upregulation precedes the  
396 transcriptional regulation, with relatively little change in mRNA abundances within the first  
397 120 min (Figure 3C-E). Many components of the classical inflammasome that are activated  
398 by *Salmonella*<sup>70</sup>, including *Nlrp3*, *Casp1* and *Gsdmd*, are among those transcriptionally  
399 upregulated after 120 min of infection with either strain of *Salmonella* (Figure S4C). This is  
400 after the initial wave of cell death (Figure 1C) that is typically attributed to inflammasome  
401 activation.

402

403 Gene ontology enrichment analysis of transcripts with differential translational efficiencies  
404 during the first 60 min of WT vs injectisome mutant *Salmonella* infection showed they have  
405 functions related to cytokine activity and, strikingly, DNA binding and transcription (Figure 3F,

406 S4D, Table S3). In contrast, and similar to previous transcriptomic studies<sup>3</sup>, the  
407 transcriptional response was also enriched for cytokines and other cell signalling genes but  
408 there was no such enrichment for DNA binding/transcription related genes. Beyond the initial  
409 60 min, genes with injectisome-dependent transcriptional induction were enriched for DNA  
410 binding functions, though the overlap with the rapidly transcriptionally regulated DNA binding  
411 factors was small (Figure S4E). Overall, this reinforces the hypothesis that rapid,  
412 injectisome-dependent translational induction of transcription modulators reshapes the  
413 transcriptional landscape, and consequently, response of macrophages to *Salmonella*  
414 infection.

415 **Discussion**

416 Cellular stress alters gene expression dynamics<sup>1–5,71,72</sup>. Here we show that bacterial infection  
417 is a potent stressor that induces selective host protein synthesis through modulating mRNA  
418 translation efficiency within the first hour of infection. Much of this regulation of translation  
419 efficiency is rapidly triggered during the interaction between the *Salmonella* injectisome and  
420 the macrophage plasmalemma, leading to the rapid synthesis of transcriptional modulators.  
421 This appears to be triggered predominately by injectisome penetration, rather than the  
422 subsequent injection of effector molecules. This study highlights the importance of cellular  
423 responses to pathogen attack, and potentially other insults, to be able to rapidly generate  
424 proteins, especially DNA binding proteins such as transcription factors, by modulating the  
425 translation efficiency of mRNA molecules in the cytoplasm. This provides a mechanism to  
426 synergize the transcriptional response to biotic stress.

427

428 We found that, in macrophages, one of the mRNAs controlled at the translational level  
429 encoded the transcription factor EGR1. EGR1 induction was shown to negatively regulate  
430 inflammation and cell death-associated genes resulting in enhanced cell survival and a  
431 limited inflammatory response. EGR1 was recently found to be involved in macrophage  
432 development by limiting the accessibility of inflammatory gene enhancers through  
433 recruitment of the NuRD chromatin remodelling machinery<sup>57</sup> and is known to be rapidly and  
434 transiently induced in response to various stimuli and has been assigned a diverse range of  
435 roles, including regulating replication and cell death<sup>54,58,59,73</sup>. Here, we revealed that  
436 accumulation of EGR1 protein is increased by a co-ordinated upregulation of translation as  
437 well as transcription. Therefore, overall synthesis of EGR1 protein is particularly rapid and  
438 robust and occurs within minutes after the bacterial injectisome interacts with the  
439 macrophage plasmalemma. The *Egr1* mRNA and EGR1 protein levels both show tight  
440 temporal control, with maximal levels at 60 and 120 min, respectively, declining to  
441 undetectable levels within 4 h post-infection. This transient induction of EGR1 protein

442 actively contributes to macrophage survival, as supported by our infection study with the  
443 EGR1<sup>KO</sup> mutant. We subsequently revealed that EGR1 acts as a transcriptional suppressor  
444 for genes associated with immune processes, including inflammatory genes such as IL-1 $\beta$ ,  
445 demonstrating the critical role of EGR1 in restraining the immune response during  
446 *Salmonella* infection. Their increased expression likely contributes to the observed increases  
447 in the rate of death of EGR1<sup>KO</sup> mutant macrophages following infection. The rapid death of  
448 *Salmonella*-infected macrophages is typically attributed to SPI-1<sup>24,25</sup>. Our data suggest that  
449 EGR1 restrains pro-inflammatory signals in WT macrophages during *Salmonella* infection,  
450 and thereby inhibits cell death<sup>74,75</sup>. While restraining inflammation likely contributes to  
451 survival of macrophages, the decrease of pro-inflammatory and pro-cell death gene  
452 expression due to transient EGR1 production appears to ultimately but inadvertently benefit  
453 the bacterial invader as evidenced by the fact most macrophages that survive injectisome-  
454 mediated infection continue to harbour viable bacteria intracellularly.

455  
456 Our data obtained with *Salmonella* cells expressing the SptP-GFP blocking substrate to  
457 inhibit T3SS-mediated effector secretion supports a model where *Egr1* upregulation at the  
458 translational and transcriptional levels is triggered by penetration of the host cell membrane  
459 by the bacterial injectisome. Recently, a model has been proposed that describes  
460 transcriptional induction following exposure to the *Candida albicans* pore forming toxin  
461 candidalysin<sup>76</sup>. We inferred that the injectisome-dependent translation and transcription of  
462 *Egr1* is activated through a similar mechanism, as supported by observations that other  
463 bacterial secretion systems require EGFR and ERK kinases for *Egr1* expression<sup>60,62</sup>.  
464 Supporting this, we show that induction of SPI-1-dependent *Egr1* expression occurs rapidly  
465 as *Salmonella* establishes its infection, in the same timeframe as the T3SS is penetrating the  
466 macrophages. We show that it is the penetration by the injectisome of the macrophage  
467 plasmalemma that is responsible for increased EGR1 expression, not the secretion of  
468 effectors.

469  
470 In summary, we have demonstrated the significance of rapid, transient reprogramming of  
471 gene expression, which is mediated primarily by increases in translation of mRNAs enriched  
472 for DNA binding proteins. Many of these are transcription factors and will therefore  
473 subsequently reshape the transcriptional landscape during the initial hour of *Salmonella*  
474 infection of macrophages. Upon encountering host macrophages, *Salmonella* swiftly boosts  
475 the expression of SPI-1 structural components, preparing for infection. Penetration of the  
476 macrophage membrane by the SPI-1 injectisome is a major trigger for the changes in host  
477 gene expression, which leads to rapid and robust protein production including that of EGR1.  
478 EGR1 is a transcriptional suppressor of immune genes and therefore transient expression of

479 EGR1 restrains the inflammatory response and host cell death. We hypothesize that  
480 *Salmonella* exploits this brief period of immunosuppression to establish infection, leading to  
481 later downregulation of cytokine expression and host survival (Figure 4). In conclusion, this  
482 work underscores the critical role of translational regulation in defining the response to  
483 bacterial pathogens and the importance of Type III injectisome penetration of host cell  
484 membranes, a neglected but crucial aspect of the host-bacterial interaction.

485 **Methods**

486 **Macrophage cell culture**

487 Primary bone marrow derived macrophages (BMDM) were harvested as previously  
488 described<sup>33</sup>. Briefly, bone marrow from the rear legs of C57BL/6 mice was extracted,  
489 suspended in culture media, and plated at a density of 10<sup>6</sup> cells/ml supplemented with  
490 20 ng/ml M-CSF (Peprotech). Cells were differentiated for 7 days, with additional M-CSF  
491 supplementation 4 days post-extraction. Immortalized bone marrow-derived macrophages  
492 (iBMDM) were generated by retroviral transformation of bone marrow-derived macrophages  
493 as previously described<sup>77</sup>. Cells were routinely grown in DMEM supplemented with 10%  
494 foetal bovine serum at 37°C, 5% CO<sub>2</sub>.

495

496 **Salmonella infection**

497 *Salmonella* Typhimurium SL1344 WT and Δ<sup>r</sup>rgJ were sub-cultured in LB from stationary  
498 phase cultures and grown at 37°C, with shaking at 200 rpm, until late exponential phase.  
499 Bacteria were washed and diluted in culture media and added to cells at a multiplicity of  
500 infection of 10. For infections using primary bone marrow-derived macrophages, all media  
501 was supplemented with 20 ng/ml M-CSF. Unless otherwise indicated, after 15 min media  
502 was supplemented with 100 µg/ml gentamicin.

503

504 **Microscopy**

505 At the indicated timepoint, cells were fixed in 4% paraformaldehyde, permeabilized and  
506 stained with Phalloidin-CF594 conjugate (Biotium), and goat anti-*Salmonella* CSA-1 (Insight  
507 Biotechnology) followed by anti-goat IgG conjugated to Alexa488 (Abcam). Cells were  
508 imaged and the proportion infected determined. Macrophages with intracellular bacteria, as  
509 determined by the intensity of CSA-1 staining and the position of *Salmonella* within the cell,  
510 were considered infected. Macrophages that were uninfected (no intracellular bacteria) but  
511 had *Salmonella* associated with the host cell surface membrane were considered to be in  
512 the process of becoming infected.

513

514 **Gentamicin protection assay**

515 The use of gentamicin protection assay to assess the number of intracellular bacterial has  
516 been described previously<sup>2</sup>. This protocol was modified to better account for host cell death.  
517 Briefly, 1 h post gentamicin treatment (i.e. 75 min post infection) macrophages were  
518 trypsinized, counted, and lysed in 0.09% Triton X-100. Serial dilutions of lysates were plated  
519 on LB-agar and grown at 37°C overnight. The *Salmonella* colonies were counted and divided  
520 by the number of counted host macrophages.

521

### 522 **Cytotoxicity assay**

523 Cytotoxicity was measured by lactate dehydrogenase release using the CytoTox 96 Non-  
524 Radioactive Cytotoxicity Assay kit (Promega) according to the manufacturer's instructions.  
525 Cytotoxicity was determined relative to total cell lysis by 0.9% Triton X-100.

526

### 527 **Ribosome profiling with parallel RNA sequencing**

528 Ribosome profiling was performed as previously described<sup>36</sup>, a schematic of which is  
529 presented in Figure 1E. Briefly, at the indicated timepoint, culture supernatant was removed  
530 from cells and flash frozen. Cells were lysed in buffer containing cycloheximide and  
531 chloramphenicol, and lysates were split for RNA-Seq and Ribo-Seq. For Ribo-Seq, lysates  
532 were treated with RNase I and fragments protected from digestion by the ribosome were  
533 purified. For RNA-Seq, total cellular RNA was fragmented by alkaline hydrolysis. This was  
534 followed by library generation as previously described<sup>36,78-80</sup>. Sequencing was performed  
535 using NextSeq-500 or 2000 (Illumina).

536

537 Reads were aligned sequentially to mouse rRNA, mouse mRNA, *Salmonella* rRNA and  
538 *Salmonella* mRNA. Mouse reference sequences were based on NCBI release mm10, and  
539 *Salmonella* reference sequences were based on GenBank sequences FQ312003.1,  
540 HE654725.1, HE654726.1 and HE654724.1. RiboSeqR<sup>36</sup> was used to confirm the quality of  
541 libraries and to count reads aligning to coding sequences. Xtail<sup>81</sup> was used to determine  
542 differential translational efficiency of these coding sequences and edgeR<sup>82</sup> was used for  
543 normalization and to filter *Salmonella* genes by expression for retention in further analysis.  
544 Gene set enrichment analysis was performed using g:Profiler<sup>83</sup>.

545

### 546 **Western immunoblotting**

547 Protein was harvested from cells disrupted with lysis buffer (50 mM Tris-HCl pH 8.0, 150 mM  
548 NaCl, 1 mM EDTA, 10% glycerol, 1% Triton X-100, 0.1% IGEPAL-CA630) containing  
549 protease (cComplete Mini, Roche) and phosphatase inhibitors (PhosSTOP, Roche). 30 µg  
550 protein was separated by SDS-PAGE and transferred to nitrocellulose membrane. EGR1  
551 was detected using rabbit anti-EGR1 (Cell Signaling) followed by anti-rabbit conjugated to

552 HRP (Cell Signaling). The HRP signal was assayed using SuperSignal West Pico PLUS  
553 substrate (Thermo Scientific). GAPDH was detected using mouse anti-GAPDH (Sigma  
554 Aldrich) followed by anti-mouse conjugated to IRDye 800 CW (Licor). SipC was detected by  
555 mouse anti-SipC (tgcBIOMICS) followed by anti-mouse IgG antibody conjugated to HRP  
556 (Promega). GroEL was detected by rabbit anti-GroEL (Abcam) followed by anti-rabbit IgG  
557 antibody conjugated to HRP (Promega). Myc tagged SptP-GFP blocking substrates were  
558 detected with anti-Myc-HRP conjugate mouse antibody (Cell Signaling).

559

560 **Reverse transcription quantitative polymerase chain reaction (RT-qPCR)**

561 RNA was extracted from cells using TRIzol (Invitrogen) per the manufacturer's instructions.  
562 Reverse transcription was performed using M-MLV reverse transcriptase (Promega) with  
563 random hexamer primers 'Promega) per the manufacturer's instructions. Realtime qPCR  
564 was performed using iTaq Universal SYBR Green Supermix (Bio-Rad) and assayed on ViiA  
565 7 system (Applied Biosystems) per the manufacturer's instructions. Primers were designed  
566 using PrimerBLAST (Table S4).

567

568 **Knockout of EGR1**

569 The Alt-R CRISPR-Cas system (IDT) was used per the manufactures instructions to edit the  
570 *Egr1* coding sequence using guide RNAs targeting *Egr1* or no genes as a negative control  
571 (Table S5)<sup>84</sup>. The system was delivered by lipofection into macrophages using Lipofectamine  
572 CRISPRMAX (Invitrogen). A clonal population was generated and targeted Sanger  
573 sequencing at the *Egr1* locus was performed (Genewiz) to confirm mutation of *Egr1*.

574

575 **Blocked injectisome *Salmonella* transformant**

576 Type III injectisomes can be blocked by fusing GFP to the C-terminus of an effector protein<sup>63</sup>.  
577 To generate our inducible blocking substrate construct, gDNA encoding the *Salmonella*  
578 chaperone SicP (residues 1-116) up to and including the downstream gene encoding the  
579 effector protein SptP (residues 1-543) was inserted into the pTrc99a plasmid<sup>85</sup> in-frame with  
580 sequence encoding C-terminal GFP followed by a myc-tag. IPTG induction results in the  
581 production of an mRNA transcript encoding wild type SicP chaperone which promotes  
582 efficient targeting of SicP's cognate substrate (in this case the SptP-GFP-myc blocking  
583 substrate) to the injectisome export machinery. The mRNA transcript also encodes the SptP-  
584 GFP-myc fusion protein which is targeted to the injectisome export machinery and stalls  
585 within the export channel, blocking the secretion of effector proteins via the SPI-1  
586 injectisome. To block effector protein secretion via the injectisome, *Salmonella* cells carrying  
587 the inducible blocking substrate construct were grow in LB containing 100 µg.ml ampicillin  
588 and expression of the blocking substrate (and the SicP chaperone) was achieved by

589 supplementing the media with isopropyl  $\beta$ -D-1-thiogalactopyranoside (IPTG) to a final  
590 concentration of 100  $\mu$ M.

591

### 592 **mRNA 3' end sequencing**

593 Preparation of mRNA 3' end sequencing libraries was performed using QuantSeq 3' mRNA-  
594 Seq Library Prep Kit (Lexogen) with TRIzol extracted RNA and libraries were sequenced by  
595 Novogene Ltd. Reads were aligned to the mouse genome (mm10) and those aligning to  
596 genes counted. Read count normalization and differential expression analysis was  
597 performed using edgeR.

598

### 599 **Enzyme-linked immunosorbent assay (ELISA)**

600 Culture supernatants were removed from infected cells at the indicated timepoint. ELISAs  
601 were performed to quantify IL-1 $\beta$  in these culture supernatants using the Mouse IL-1 beta/IL-  
602 1F2 DuoSet ELISA kit (R&D Systems) per the manufacturer's instructions.

603

### 604 **Protein export assays**

605 Export assays were performed as previously described<sup>86</sup>. Briefly, *Salmonella* strains were  
606 cultured at 37 °C in LB broth with 100  $\mu$ M IPTG to mid-log phase (OD600nm 1.5) for 2 h.  
607 Cells were centrifuged (6000 x g, 3 min) and resuspended in fresh media and grown for a  
608 further 60 min at 37 °C. The cells were pelleted by centrifugation (16,000 x g, 5 min) and the  
609 supernatant passed through a 0.2  $\mu$ m nitrocellulose filter. Proteins were precipitated with  
610 10% trichloroacetic acid (TCA) and 1% Triton X-100 on ice for 1 hr, pelleted by centrifugation  
611 (16,000 x g, 10 min), washed with ice-cold acetone, and resuspended in SDS-PAGE loading  
612 buffer (volumes calibrated according to cell densities). Fractions were analyzed by  
613 immunoblotting with anti-SipC (tgcBIOMICS), anti-Myc (Cell Signaling) and anti-GroEL  
614 (Abcam) anti-sera.

615

### 616 **Data availability.**

617 Raw and processed data are available from ArrayExpress accessions E-MTAB-13212 and  
618 E-MTAB-13213 or can be found in the supplementary tables. Customized scripts used for  
619 this project are available upon request.

620

### 621 **Conflict of interest:**

622 The authors declare no conflict of interest

623

624 **Acknowledgements:**

625 We would also like to thank Jim Kaufman, Klaus Okkenhaug, and Alex Murphy for  
626 discussions and comments on the manuscript. F.L. was supported by a BBSRC DTP  
627 studentship. G.W. was supported by the Department of Pathology PhD studentship,  
628 B.Y.W.C., R.J. and M.B. and O.J.B. are supported by a Medical Research Council  
629 Fellowship to B.Y.W.C. [MR/R021821/1]. J.P. and M.B. are supported by a BBSRC project  
630 grant awarded to B.Y.W.C. [BB/V006096/1]. The B.Y.W.C. laboratory is supported by a  
631 Medical Research Council Fellowship [MR/R021821/1], BBSRC project grants  
632 [BB/X001261/1, BB/V017780/1 and BB/V006096/1] and a Royal Society Research Grant  
633 [RGS\R2\192222]. Figures created with BioRender.com.

634

635 **Author contributions:**

636 B.Y.W.C. conceived the research. B.Y.W.C., G.W., R.J., J.P., O.J.B., F.L., J.P.C. and C.B.  
637 designed experiments. R.J., J.P. and B.Y.W.C. generated RiboSeq, RNA-Seq and QuantSeq  
638 libraries. G.W., R.J. and J.P. performed molecular and cell biology experiments. O.J.B.  
639 generated *Salmonella* mutants. F.L. performed bacterial bioinformatics. B.Y.W.C., G.W., R.J.,  
640 J.P., F.L. and M.B. performed the bioinformatic analysis. C.B. provided macrophages and  
641 *prgJ* mutant. P.T. provided training for extracting BMDM. B.Y.W.C., G.W., O.J.B. and J.P.C.  
642 wrote the manuscript.

643

644 **Figure Legends**

645 **Fig 1:** *Salmonella* SPI-1 dependent infection rapidly alters macrophage translation. **(A)** Mock  
646 infected and WT *Salmonella* infected macrophages 5 min post infection. Actin is shown in  
647 red, and *Salmonella* are shown in green. Arrows indicate *Salmonella* associated with the cell  
648 membrane. **(B)** Percentage of macrophages affected by WT *Salmonella* during the first 15  
649 min of infection determined by immunofluorescent microscopy. Infected cells contain  
650 intracellular *Salmonella* infecting cells do not but have *Salmonella* associated with the host  
651 cell membrane,  $n=3$ . **(C)** *Salmonella* colony forming units (CFU) recovered 75 min post WT  
652 and SPI-1 deficient ( $\Delta prgJ$ ) *Salmonella* infection per host macrophage. Significance  
653 determined by Student's t-test;  $n=2$ . **(D)** Cytotoxicity of WT or  $\Delta prgJ$  *Salmonella* or mock  
654 infection of macrophages as determined by lactate dehydrogenase (LDH) release into  
655 culture supernatant. Significance determined by Students t-test;  $n=2$ . **(E)** Experimental  
656 outline detailing the preparation of ribosome profiling and RNA-Seq libraries from infected  
657 macrophages. Details are provided in the materials and methods (RPF: ribosome-protected  
658 RNA fragments, NGS: next-generation sequencing). **(F)** Diagram illustrating the relationship  
659 between mRNA abundance (measured by RNA-Seq), protein synthesis (measured by Ribo-

660 Seq) and translational efficiency (TE). **(G)** Comparison of changes in mRNA abundance (left)  
661 and TE (right) on infection with WT or  $\Delta prgJ$  *Salmonella* over mock infection. Genes  
662 upregulated transcriptionally in both ( $\log_2 FC > 1$ ) are shown in red. **(H)** Heatmap showing  
663 mRNA abundance, protein synthesis and TE of transcriptionally upregulated genes  
664 highlighted in G. Genes are ordered by hierarchical clustering of mRNA abundance across  
665 all conditions (left) **(I)** Ribo-Seq and RNA-Seq coverage of *Tnf* and *Zfp36* transcripts, which  
666 are known to have increased TE on exposure to bacterial PAMPs. Ribo-Seq reads are  
667 represented by their P site position and colored by their reading frame relative to the start  
668 codon of the coding sequence, represented by the bar above each plot with the start and  
669 stop positions indicated on the x-axis. *Rpl4* is presented as a control gene expressed in all  
670 samples. Significance determined using Xtail as described in the Materials and Methods **(J)**  
671 Normalized mRNA abundance, protein synthesis and TE of genes with  $\log_2 FC$  in TE of WT  
672 over  $\Delta prgJ$  infected macrophages greater than 1.5 and at least 50 normalized Ribo-Seq  
673 counts in WT infection. Genes are ordered by hierarchical clustering of TE across all  
674 conditions (left). Genes with low read counts (i.e. those with normalized RNA-Seq and Ribo-  
675 Seq counts less than 5) are considered lowly expressed and therefore TE cannot be reliably  
676 calculated. **(K)** Ribo-Seq and RNA-Seq transcript coverage of *Egr1*, *Il1b* and *Nr4a1* as in **G**.  
677

678 **Fig 2:** *Egr1* is rapidly induced in *Salmonella* infection to restrict expression of immune  
679 response genes. **(A)** mRNA abundance, protein synthesis and translational efficiency (TE) of  
680 *Egr1* from Fig 1K. For conditions with low *Egr1* expression TE cannot be reliably calculated  
681 (grey bar); significance determined using Xtail as described in the Materials and Methods.  
682 **(B)** *Egr1* transcript abundance over WT and SPI-1 deficient mutant ( $\Delta prgJ$ ) infection,  
683 normalized to the housekeeping gene *Supt16* and relative to cells prior to infection,  $n=2$ . **(C)**  
684 Quantification of EGR1 abundance from **D** normalized to GAPDH. **(D)** Immunoblot following  
685 EGR1 and GAPDH protein abundance across WT and  $\Delta prgJ$  infection. An equal amount of  
686 cellular protein was loaded per lane. **(E)** Experimental outline illustrating the effect of the  
687 SptP-GFP injectisome blocking substrate on protein export via the injectisome. *Salmonella*  
688 cells not producing the blocking substrate can transport effector proteins into host cells  
689 (unobstructed injectisome, left). *Salmonella* cells expressing the injectisome blocking  
690 substrate before infection are unable to transport effector subunits via the injectisome (pre-  
691 blocked injectisome, middle). *Salmonella* cells were also incubated with macrophages for 5  
692 min before inducing expression of the injectisome blocking substrate such that injectisomes  
693 can engage with macrophage cells but secretion of effectors proteins from *Salmonella* into  
694 macrophages are blocked at 5 min (injectisome blocked at 5 min, right). **(F)** Secretion  
695 analysis of WT *Salmonella* either expressing the SptP-GFP injectisome blocking subunit or  
696 carrying empty vector. Whole cell (cell) and secreted proteins (sec) from late-exponential-

697 phase cultures were separated by SDS-PAGE and immunoblotted with anti-Myc-tag (SptP-  
698 GFP), anti-SipC or anti-GroEL antisera. (G) *Egr1* transcript abundance over the *Salmonella*  
699 infection time course with blockade of the SPI-1 injectisome induced at various timepoints.  
700 Significance determined by one-sided Student's t-test;  $n=2$ . (H) Immunoblot showing EGR1  
701 expression in EGR1<sup>WT</sup> and EGR1<sup>KO</sup> macrophages infected with WT *Salmonella* at 120 min  
702 post infection. (I) Cytotoxicity of WT or mock infection of EGR1<sup>WT</sup> and EGR1<sup>KO</sup> macrophages  
703 as determined by lactate dehydrogenase (LDH) release into culture supernatant. (J) IL-1 $\beta$   
704 concentration in culture supernatant from infected EGR1<sup>KO</sup> and EGR1<sup>WT</sup> macrophages.  $n=2$   
705 except for 240 min WT *Salmonella* infection where  $n=3$  for EGR1<sup>WT</sup> and 4 for EGR1<sup>KO</sup>;  
706 significance determined using one-sided Student's t-test. (K) Normalized mRNA abundance  
707 of transcripts upregulated ( $\log_2\text{FC} > 2$ ) in EGR1<sup>KO</sup> when compared to EGR1<sup>WT</sup> macrophages  
708 at any timepoint in WT *Salmonella* infection. Genes are ordered by hierarchical clustering  
709 (left). (L) The 10 most significantly enriched gene ontology biological process terms in genes  
710 identified in J.

711  
712 **Fig 3:** Time resolved RiboSeq reveals dynamic changes in host and bacterial translation.  
713 Data from two replicates. (A) Outline of infection time course. Primary bone marrow-derived  
714 macrophages were generated from mice and infected with WT or  $\Delta\text{prgJ}$  mutant *Salmonella*.  
715 Gentamicin was used to kill extracellular bacteria at 15 min and its concentration was  
716 reduced after 1 h. (B) Transient expression dynamics of select WT *Salmonella* genes at  
717 different optical densities (OD) and over 4 h of macrophage infection, at the level of mRNA  
718 abundance, protein synthesis and translation efficiency. (C) Differential regulation of host  
719 gene expression as measured by the  $\log_2\text{FC}$  of translational efficiency (TE) vs  $\log_2\text{FC}$  mRNA  
720 abundance in WT *Salmonella* infection over  $\Delta\text{prgJ}$  infection. Dashed orange lines show the  
721  $\log_2\text{FC}$  cutoffs ( $\pm 2$ ) used to select differentially expressed genes, and genes that pass these  
722 thresholds are colored. Only genes with  $\log_2\text{FC}$  in mRNA and TE between -5 and 5 are  
723 shown here (see Fig S4B for uncropped plots). (D and E) Number of genes differentially  
724 expressed between WT and  $\Delta\text{prgJ}$  *Salmonella* infection at both the TE (D) and mRNA (E)  
725 levels. (F) Top 10 enriched GO molecular function terms in differentially expressed genes at  
726 both the TE (right) and mRNA (left) levels. Genes were split by when they were differentially  
727 expressed: at or before 60 min, and after 60 min post infection.

728  
729 **Fig 4:** Summary and model. Specific classes of *Salmonella* genes are transiently expressed  
730 as infection is established, including rapid upregulation of SPI-1 genes as bacteria encounter  
731 host macrophages, leading to increased production of T3SS injectisomes as shown.  
732 *Salmonella* SPI-1 injectisome assembly forms transient pores in the host membrane which  
733 activates host signaling pathways, leading to increased *Egr1* transcription and enhanced

734 translation. EGR1 negatively modulates immune gene transcription and, in doing so,  
735 inflammatory cytokine production in response to *Salmonella* infection is restrained, as is host  
736 cell death.

737

738 **Fig S1:** (A) Percentage of macrophages infected by WT *Salmonella* determined by  
739 microscopy at 15 and 60 min, with and without addition of gentamicin at 15 min. Significance  
740 determined by Student's t-test;  $n=2$ . (B) Percentage of macrophages infected by WT or  
741  $\Delta prgJ$  *Salmonella* determined by microscopy at 15 min. Significance determined by  
742 Student's t-test;  $n=2$ . (C) Meta-gene translatome from ribosome profiling of *Salmonella*  
743 infected macrophages at 60 min. Histograms of RPF 5' ends relative to start and stop  
744 codons colored by their reading frame relative to the coding sequence. (D) Heatmap  
745 showing mRNA abundance, protein synthesis and TE of all genes in Fig 1G. Genes are  
746 ordered by hierarchical clustering of mRNA abundance across all conditions (left). Arrows  
747 indicate direction of differential transcript abundance ( $\log_2 FC \pm 1$ ) in the indicated infection vs  
748 mock.  
749 (E) Ribo-Seq and RNA-Seq transcript coverage of *Atf4*. Ribo-Seq reads are represented by  
750 their P site position and colored by their reading frame relative to the start codon of the main  
751 *Atf3* coding sequence. Open reading frames are represented by bars above each plot. (F)  
752 Comparison of changes in mRNA abundance (left) and TE (right) on infection with WT over  
753 mock infection or  $\Delta prgJ$  *Salmonella*. Genes upregulated transcriptionally in both ( $\log_2 FC > 1$ )  
754 are shown in red. *Egr1*, *Nr4a1* and *Nfkbia* are plotted separately due to low abundance in  
755 mock infection precluding accurate calculation of TE, and as such TE fold change in WT  
756 *Salmonella* over mock infection. (G) Normalised mRNA abundance and protein synthesis of  
757 *Nlrp3* at 60 min post-infection. (H) Ribo-Seq and RNA-Seq transcript coverage of *Nlrp3* as in  
758 E. The *Nlrp3* uORF can be readily seen as reads in a different reading frame within the 5'  
759 UTR.

760

761 **Fig S2:** (A) Example section of the *Egr1* coding sequence with an alignment from targeted  
762 sequencing of the *Egr1* locus in the EGR1 KO macrophages. Mismatched bases and  
763 deletions are highlighted in red. (B) Principal component analysis of the transcriptomes of  
764 WT *Salmonella* infected or mock infected EGR1 KO or control macrophages over an  
765 infection time course.

766

767 **Fig S3:** (A) Percentage of primary macrophages infected by WT or  $\Delta prgJ$  *Salmonella*  
768 determined by microscopy at 15 min. (B) Meta-gene translatome from ribosome profiling  
769 across a *Salmonella* primary bone marrow derived macrophage infection time course.

770 Histograms of RPF 5' ends relative to start and stop codons colored by their reading frame  
771 relative to the coding sequence.

772

773 **Fig S4:** (A)  $\log_2$ FC TE vs  $\log_2$ FC mRNA abundance between the indicated infections, across  
774 the time course. Dashed orange lines show the  $\log_2$ FC cutoffs ( $\pm 2$ ) used to select  
775 differentially expressed genes; genes that pass these thresholds are colored. (B) Number of  
776 genes differentially expressed between WT vs mock and  $\Delta$ p<sub>rgJ</sub> vs mock infection at both the  
777 TE (right) and mRNA (left) levels. (C) Expression of genes encoding components of the  
778 inflammasome<sup>70</sup> that are upregulated over the infection timecourse. (D) Top 10 enriched GO  
779 molecular function terms in differentially expressed genes at both the TE (right) and mRNA  
780 (left) levels. Genes were split by when they were differentially expressed: at or before 60  
781 min, and after 60 min post infection. (E) Overlap of genes with DNA binding and transcription  
782 related annotations that are differentially regulated on the translational level at or before 60  
783 min or the transcriptional level after 60 min in the comparison of WT vs  $\Delta$ p<sub>rgJ</sub> infection.

784

## 785 **References**

- 786 1. Denzer, L., Schrotten, H., and Schwerk, C. (2020). From gene to protein - how  
787 bacterial virulence factors manipulate host gene expression during infection. *Int. J.*  
788 *Mol. Sci.* 21, 3730. 10.3390/ijms21103730.
- 789 2. Hannemann, S., Gao, B., and Galán, J.E. (2013). *Salmonella* modulation of host cell  
790 gene expression promotes its intracellular growth. *PLoS Pathog.* 9, e1003668.  
791 10.1371/journal.ppat.1003668.
- 792 3. Jensen, K., Gallagher, I.J., Kaliszewska, A., Zhang, C., Abejide, O., Gallagher, M.P.,  
793 Werling, D., and Glass, E.J. (2016). Live and inactivated *Salmonella enterica* serovar  
794 Typhimurium stimulate similar but distinct transcriptome profiles in bovine  
795 macrophages and dendritic cells. *Vet. Res.* 47. 10.1186/s13567-016-0328-y.
- 796 4. Ordas, A., Hegedus, Z., Henkel, C. V, Stockhammer, O.W., Butler, D., Jansen, H.J.,  
797 Racz, P., Mink, M., Spaink, H.P., and Meijer, A.H. (2011). Deep sequencing of the  
798 innate immune transcriptomic response of zebrafish embryos to *Salmonella* infection.  
799 *Fish Shellfish Immunol.* 31, 716–724. 10.1016/j.fsi.2010.08.022.
- 800 5. Maekawa, S., Wang, P.C., and Chen, S.C. (2019). Comparative study of immune  
801 reaction against bacterial infection from transcriptome analysis. *Front. Immunol.* 10.  
802 10.3389/fimmu.2019.00153.
- 803 6. Westermann, A.J., Venturini, E., Sellin, M.E., Förstner, K.U., Hardt, W.D., and Vogel,  
804 J. (2019). The major RNA-binding protein ProQ impacts virulence gene expression in



838 1658. 10.1126/science.287.5458.1655.

839 17. Guignot, J., and Tran Van Nhieu, G. (2016). Bacterial control of pores induced by the  
840 type III secretion system: mind the gap. *Front. Immunol.* 7, 84.  
841 10.3389/fimmu.2016.00084.

842 18. Park, D., Lara-Tejero, M., Waxham, M.N., Li, W., Hu, B., Galán, J.E., and Liu, J.  
843 (2018). Visualization of the type III secretion mediated salmonella–host cell interface  
844 using cryo-electron tomography. *Elife* 7. 10.7554/ELIFE.39514.

845 19. Murthy, S., Karkossa, I., Schmidt, C., Hoffmann, A., Hagemann, T., Rothe, K., Seifert,  
846 O., Anderegg, U., von Bergen, M., Schubert, K., et al. (2022). Danger signal  
847 extracellular calcium initiates differentiation of monocytes into SPP1/osteopontin-  
848 producing macrophages. *Cell Death Dis.* 2022 131 13, 1–15. 10.1038/s41419-022-  
849 04507-3.

850 20. Koumangoye, R. (2022). The role of Cl- and K+ efflux in NLRP3 inflammasome and  
851 innate immune response activation. *Am. J. Physiol. - Cell Physiol.* 322, C645–C652.  
852 10.1152/AJPCELL.00421.2021/ASSET/IMAGES/LARGE/AJPCELL.00421.2021\_F00  
853 2.jpeg.

854 21. Richter-Dahlfors, A., Buchan, A.M.J., and Finlay, B.B. (1997). Murine salmonellosis  
855 studied by confocal microscopy: *Salmonella Typhimurium* resides intracellularly inside  
856 macrophages and exerts a cytotoxic effect on phagocytes *in vivo*. *J. Exp. Med.* 186,  
857 569–580. 10.1084/jem.186.4.569.

858 22. Price, J. V., and Vance, R.E. (2014). The macrophage paradox. *Immunity* 41, 685–  
859 693. 10.1016/j.immuni.2014.10.015.

860 23. Talbot, S., Tötemeyer, S., Yamamoto, M., Akira, S., Hughes, K., Gray, D., Barr, T.,  
861 Mastroeni, P., Maskell, D.J., and Bryant, C.E. (2009). Toll-like receptor 4 signalling  
862 through MyD88 is essential to control *Salmonella enterica* serovar *Typhimurium*  
863 infection, but not for the initiation of bacterial clearance. *Immunology* 128, 472.  
864 10.1111/J.1365-2567.2009.03146.X.

865 24. Grant, A.J., Sheppard, M., Deardon, R., Brown, S.P., Foster, G., Bryant, C.E.,  
866 Maskell, D.J., and Mastroeni, P. (2008). Caspase-3-dependent phagocyte death  
867 during systemic *Salmonella enterica* serovar *Typhimurium* infection of mice.  
868 *Immunology* 125, 28–37. 10.1111/j.1365-2567.2008.02814.x.

869 25. Gram, A.M., Wright, J.A., Pickering, R.J., Lam, N.L., Booty, L.M., Webster, S.J., and  
870 Bryant, C.E. (2021). *Salmonella* flagellin activates NAIP/NLRC4 and canonical NLRP3  
871 inflammasomes in human macrophages. *J. Immunol.* 206, 631–640.

872 10.4049/jimmunol.2000382.

873 26. Bergsbaken, T., Fink, S.L., and Cookson, B.T. (2009). Pyroptosis: host cell death and  
874 inflammation. *Nat. Rev. Microbiol.* 7, 99–109. 10.1038/nrmicro2070.

875 27. Chen, L.M., Kaniga, K., and Galán, J.E. (1996). *Salmonella* spp. are cytotoxic for  
876 cultured macrophages. *Mol. Microbiol.* 21, 1101–1115. 10.1046/j.1365-  
877 2958.1996.471410.x.

878 28. Monack, D.M., Raupach, B., Hromockyj, A.E., and Falkow, S. (1996). *Salmonella*  
879 *Typhimurium* invasion induces apoptosis in infected macrophages. *PNAS* 93, 9833–  
880 9838. 10.1073/pnas.93.18.9833.

881 29. Lundberg, U., Vinatzer, U., Berdnik, D., von Gabain, A., and Baccarini, M. (1999).  
882 Growth phase-regulated induction of *Salmonella*-induced macrophage apoptosis  
883 correlates with transient expression of SPI-1 genes. *J. Bacteriol.* 181, 3433–3437.  
884 10.1128/JB.181.11.3433-3437.1999.

885 30. Wang, L., Trebicka, E., Fu, Y., Waggoner, L., Akira, S., Fitzgerald, K.A., Kagan, J.C.,  
886 and Cherayil, B.J. (2011). Regulation of lipopolysaccharide-induced translation of  
887 tumor necrosis factor-alpha by the toll-like receptor 4 adaptor protein TRAM. *J. Innate*  
888 *Immun.* 3, 437–446. 10.1159/000324833.

889 31. Dumitru, C.D., Ceci, J.D., Tsatsanis, C., Kontoyiannis, D., Stamatakis, K., Lin, J.-H.,  
890 Patriotis, C., Jenkins, N.A., Copeland, N.G., Kollias, G., et al. (2000). TNF- $\alpha$  Induction  
891 by LPS Is Regulated Posttranscriptionally via a Tpl2/ERK-Dependent Pathway. *Cell*  
892 103, 1071–1083. 10.1016/S0092-8674(00)00210-5.

893 32. Drecktrah, D., Knodler, L.A., Ireland, R., and Steele-Mortimer, O. (2006). The  
894 mechanism of *Salmonella* entry determines the vacuolar environment and intracellular  
895 gene expression. *Traffic* 7, 39–51. 10.1111/J.1600-0854.2005.00360.X.

896 33. Man, S.M., Hopkins, L.J., Nugent, E., Cox, S., Glück, I.M., Tourlomousis, P., Wright,  
897 J.A., Cicuta, P., Monie, T.P., and Bryant, C.E. (2014). Inflammasome activation  
898 causes dual recruitment of NLRC4 and NLRP3 to the same macromolecular complex.  
899 *Proc. Natl. Acad. Sci.* 111, 7403–7408. 10.1073/PNAS.1402911111.

900 34. Fink, S.L., and Cookson, B.T. (2007). Pyroptosis and host cell death responses during  
901 *Salmonella* infection. *Cell. Microbiol.* 9, 2562–2570. 10.1111/J.1462-  
902 5822.2007.01036.X.

903 35. Ingolia, N.T., Ghaemmaghami, S., Newman, J.R.S., and Weissman, J.S. (2009).  
904 Genome-wide analysis in vivo of translation with nucleotide resolution using ribosome

905 profiling. *Science* 324, 218–223. 10.1126/SCIENCE.1168978.

906 36. Chung, B.Y., Hardcastle, T.J., Jones, J.D., Irigoyen, N., Firth, A.E., Baulcombe, D.C.,  
907 and Brierley, I. (2015). The use of duplex-specific nuclease in ribosome profiling and a  
908 user-friendly software package for Ribo-seq data analysis. *RNA* 21, 1731.  
909 10.1261/RNA.052548.115.

910 37. Vattem, K.M., and Wek, R.C. (2004). Reinitiation involving upstream ORFs regulates  
911 ATF4 mRNA translation in mammalian cells. *Proc. Natl. Acad. Sci.* 101, 11269–  
912 11274. 10.1073/pnas.0400541101.

913 38. Landmann, R., Knopf, H.P., Link, S., Sansano, S., Schumann, R., and Zimmerli, W.  
914 (1996). Human monocyte CD14 is upregulated by lipopolysaccharide. *Infect. Immun.*  
915 64, 1762–1769. 10.1128/IAI.64.5.1762-1769.1996.

916 39. Yang, H., Li, Q., Stroup, E.K., Wang, S., and Ji, Z. (2024). Widespread stable  
917 noncanonical peptides identified by integrated analyses of ribosome profiling and  
918 ORF features. *Nat. Commun.* 2024 151 15, 1–18. 10.1038/s41467-024-46240-9.

919 40. Bryant, C. (2021). Inflammasome activation by *Salmonella*. *Curr. Opin. Microbiol.* 64,  
920 27–32. 10.1016/j.mib.2021.09.004.

921 41. Qu, Y., Misaghi, S., Newton, K., Maltzman, A., Izrael-Tomasevic, A., Arnott, D., and  
922 Dixit, V.M. (2016). NLRP3 recruitment by NLRC4 during *Salmonella* infection. *J. Exp.*  
923 *Med.* 213, 877–885. 10.1084/JEM.20132234.

924 42. Li, P., Allen, H., Banerjee, S., Franklin, S., Herzog, L., Johnston, C., McDowell, J.,  
925 Paskind, M., Rodman, L., Salfeld, J., et al. (1995). Mice deficient in IL-1 beta-  
926 converting enzyme are defective in production of mature IL-1 beta and resistant to  
927 endotoxic shock. *Cell* 80, 401–411. 10.1016/0092-8674(95)90490-5.

928 43. Hersh, D., Monack, D.M., Smith, M.R., Ghori, N., Falkow, S., and Zychlinsky, A.  
929 (1999). The *Salmonella* invasin SipB induces macrophage apoptosis by binding to  
930 caspase-1. *Proc. Natl. Acad. Sci.* 96, 2396–2401. 10.1073/pnas.96.5.2396.

931 44. Cook, P., Tötemeyer, S., Stevenson, C., Fitzgerald, K.A., Yamamoto, M., Akira, S.,  
932 Maskell, D.J., and Bryant, C.E. (2007). *Salmonella*-induced SipB-independent cell  
933 death requires Toll-like receptor-4 signalling via the adapter proteins Tram and Trif.  
934 *Immunology* 122, 222. 10.1111/J.1365-2567.2007.02631.X.

935 45. Reyes Ruiz, V.M., Ramirez, J., Naseer, N., Palacio, N.M., Siddarthan, I.J., Yan, B.M.,  
936 Boyer, M.A., Pensinger, D.A., Sauer, J.-D., and Shin, S. (2017). Broad detection of  
937 bacterial type III secretion system and flagellin proteins by the human NAIP/NLRC4

938 inflammasome. Proc. Natl. Acad. Sci. 114, 13242–13247. 10.1073/pnas.1710433114.

939 46. Mariathasan, S., Newton, K., Monack, D.M., Vucic, D., French, D.M., Lee, W.P.,  
940 Roose-Girma, M., Erickson, S., and Dixit, V.M. (2004). Differential activation of the  
941 inflammasome by caspase-1 adaptors ASC and Ipaf. Nature 430, 213–218.  
942 10.1038/nature02664.

943 47. Martin-Sanchez, F., Diamond, C., Zeitler, M., Gomez, A.I., Baroja-Mazo, A., Bagnall,  
944 J., Spiller, D., White, M., Daniels, M.J.D., Mortellaro, A., et al. (2016). Inflammasome-  
945 dependent IL-1 $\beta$  release depends upon membrane permeabilisation. Cell Death  
946 Differ. 23, 1219–1231. 10.1038/cdd.2015.176.

947 48. Lau, L.F., and Nathans, D. (1987). Expression of a set of growth-related immediate  
948 early genes in BALB/c 3T3 cells: coordinate regulation with c-fos or c-myc. Proc. Natl.  
949 Acad. Sci. 84, 1182–1186. 10.1073/PNAS.84.5.1182.

950 49. McMahon, S.B., and Monroe, J.G. (1996). The role of early growth response gene 1  
951 (egr-1) in regulation of the immune response. J. Leukoc. Biol. 60, 159–166.  
952 10.1002/jlb.60.2.159.

953 50. Bahrami, S., and Drabløs, F. (2016). Gene regulation in the immediate-early response  
954 process. Adv. Biol. Regul. 62, 37–49. 10.1016/J.JBIOR.2016.05.001.

955 51. Hamers, A.A.J., van Dam, L., Teixeira Duarte, J.M., Vos, M., Marinković, G., van Tiel,  
956 C.M., Meijer, S.L., van Stalborch, A.-M., Huvemeers, S., te Velde, A.A., et al. (2015).  
957 Deficiency of nuclear receptor Nur77 aggravates mouse experimental colitis by  
958 increased NF $\kappa$ B activity in macrophages. PLoS One 10, e0133598.  
959 10.1371/journal.pone.0133598.

960 52. Li, L., Liu, Y., Chen, H., Li, F., Wu, J., Zhang, H., He, J., Xing, Y., Chen, Y., Wang, W.,  
961 et al. (2015). Impeding the interaction between Nur77 and p38 reduces LPS-induced  
962 inflammation. Nat. Chem. Biol. 11, 339–346. 10.1038/nchembio.1788.

963 53. Partyka, J., Henkel, M., Campfield, B.T., and 14, P.A. (2020). A Novel Role for the  
964 Nuclear Receptor, NR4A1, in Klebsiella pneumoniae Lung Infection. bioRxiv,  
965 2020.09.03.282475. 10.1101/2020.09.03.282475.

966 54. Thiel, G., and Cibelli, G. (2002). Regulation of life and death by the zinc finger  
967 transcription factor Egr-1. J. Cell. Physiol. 193, 287–292. 10.1002/jcp.10178.

968 55. Chbicheb, S., Yao, X., Rodeau, J.-L., Salamone, S., Boisbrun, M., Thiel, G., Spohn,  
969 D., Grillier-Vuissoz, I., Chapleur, Y., Flament, S., et al. (2011). EGR1 expression: A  
970 calcium and ERK1/2 mediated PPAR $\gamma$ -independent event involved in the

971 antiproliferative effect of 15-deoxy- $\Delta$ 12,14-prostaglandin J2 and thiazolidinediones in  
972 breast cancer cells. *Biochem. Pharmacol.* **81**, 1087–1097. 10.1016/j.bcp.2011.02.006.

973 56. Banerji, R., and Saroj, S.D. (2021). Early growth response 1 (EGR1) activation in  
974 initial stages of host–pathogen interactions. *Mol. Biol. Rep.* **48**, 2935–2943.  
975 10.1007/s11033-021-06305-0.

976 57. Trizzino, M., Zucco, A., Deliard, S., Wang, F., Barbieri, E., Veglia, F., Gabrilovich, D.,  
977 and Gardini, A. (2021). EGR1 is a gatekeeper of inflammatory enhancers in human  
978 macrophages. *Sci. Adv.* **7**. 10.1126/sciadv.aaz8836.

979 58. Kimura, T.E., Duggirala, A., Hindmarch, C.C.T., Hewer, R.C., Cui, M.Z., Newby, A.C.,  
980 and Bond, M. (2014). Inhibition of Egr1 expression underlies the anti-mitogenic effects  
981 of cAMP in vascular smooth muscle cells. *J. Mol. Cell. Cardiol.* **72**, 9–19.  
982 10.1016/j.yjmcc.2014.02.001.

983 59. Sukhatme, V.P., Cao, X., Chang, L.C., Tsai-Morris, C.H., Stamenkovich, D., Ferreira,  
984 P.C.P., Cohen, D.R., Edwards, S.A., Shows, T.B., Curran, T., et al. (1988). A zinc  
985 finger-encoding gene coregulated with c-fos during growth and differentiation, and  
986 after cellular depolarization. *Cell* **53**, 37–43. 10.1016/0092-8674(88)90485-0.

987 60. de Grado, M., Rosenberger, C.M., Gauthier, A., Vallance, B.A., and Finlay, B.B.  
988 (2001). Enteropathogenic *Escherichia coli* infection induces expression of the early  
989 growth response factor by activating mitogen-activated protein kinase cascades in  
990 epithelial cells. *Infect. Immun.* **69**, 6217–6224. 10.1128/IAI.69.10.6217-6224.2001.

991 61. Shin, H., and Cornelis, G.R. (2007). Type III secretion translocation pores of *Yersinia*  
992 *enterocolitica* trigger maturation and release of pro-inflammatory IL-1 $\beta$ . *Cell. Microbiol.*  
993 **9**, 2893–2902. 10.1111/j.1462-5822.2007.01004.x.

994 62. Keates, S., Keates, A.C., Nath, S., Peek, R.M., and Kelly, C.P. (2005).  
995 Transactivation of the epidermal growth factor receptor by cag+ *Helicobacter pylori*  
996 induces upregulation of the early growth response gene Egr-1 in gastric epithelial  
997 cells. *Gut* **54**, 1363–1369. 10.1136/gut.2005.066977.

998 63. Radics, J., Königsmaier, L., and Marlovits, T.C. (2013). Structure of a pathogenic type  
999 3 secretion system in action. *Nat. Struct. Mol. Biol.* **2013** **21** **21**, 82–87.  
1000 10.1038/nsmb.2722.

1001 64. Kudryashev, M., Diepold, A., Amstutz, M., Armitage, J.P., Stahlberg, H., and Cornelis,  
1002 G.R. (2015). *Yersinia enterocolitica* type III secretion injectisomes form regularly  
1003 spaced clusters, which incorporate new machines upon activation. *Mol. Microbiol.* **95**,  
1004 875–884. 10.1111/MMI.12908/SUPPINFO.

1005 65. Eriksson, S., Lucchini, S., Thompson, A., Rhen, M., and Hinton, J.C.D. (2003).  
1006 Unravelling the biology of macrophage infection by gene expression profiling of  
1007 intracellular *Salmonella enterica*. *Mol. Microbiol.* 47, 103–118. 10.1046/j.1365-  
1008 2958.2003.03313.x.

1009 66. Sri Kumar, S., Kröger, C., Hébrard, M., Colgan, A., Owen, S. V., Sivasankaran, S.K.,  
1010 Cameron, A.D.S., Hokamp, K., and Hinton, J.C.D. (2015). RNA-seq brings new  
1011 insights to the intra-macrophage transcriptome of *Salmonella Typhimurium*. *PLOS*  
1012 *Pathog.* 11, e1005262. 10.1371/journal.ppat.1005262.

1013 67. Chakraborty, S., Mizusaki, H., and Kenney, L.J. (2015). A FRET-based DNA  
1014 biosensor tracks OmpR-dependent acidification of *Salmonella* during macrophage  
1015 infection. *PLOS Biol.* 13, e1002116. 10.1371/journal.pbio.1002116.

1016 68. Pérez-Morales, D., Banda, M.M., Chau, N.Y.E., Salgado, H., Martínez-Flores, I.,  
1017 Ibarra, J.A., Ilyas, B., Coombes, B.K., and Bustamante, V.H. (2017). The  
1018 transcriptional regulator SsrB is involved in a molecular switch controlling virulence  
1019 lifestyles of *Salmonella*. *PLOS Pathog.* 13, e1006497. 10.1371/journal.ppat.1006497.

1020 69. Brown, N.F., Rogers, L.D., Sanderson, K.L., Gouw, J.W., Hartland, E.L., and Foster,  
1021 L.J. (2014). A horizontally acquired transcription factor coordinates *Salmonella*  
1022 adaptations to host microenvironments. *MBio* 5, 1727–1741. 10.1128/mBio.01727-14.

1023 70. Bryant, C. (2021). Inflammasome activation by *Salmonella*. *Curr. Opin. Microbiol.* 64,  
1024 27–32. 10.1016/j.mib.2021.09.004.

1025 71. Advani, V.M., and Ivanov, P. (2019). Translational control under stress: reshaping the  
1026 translatome. *BioEssays* 41, e1900009. 10.1002/BIES.201900009.

1027 72. Hoang, H.D., Neault, S., Pelin, A., and Alain, T. (2021). Emerging translation  
1028 strategies during virus–host interaction. *Wiley Interdiscip. Rev. RNA* 12.  
1029 10.1002/WRNA.1619.

1030 73. Yan, S.F., Fujita, T., Lu, J., Okada, K., Shan Zou, Y., Mackman, N., Pinsky, D.J., and  
1031 Stern, D.M. (2000). Egr-1, a master switch coordinating upregulation of divergent  
1032 gene families underlying ischemic stress. *Nat. Med.* 6, 1355–1361. 10.1038/82168.

1033 74. Hughes, S.A., Lin, M., Weir, A., Huang, B., Xiong, L., Chua, N.K., Pang, J.,  
1034 Santavanond, J.P., Tixeira, R., Doerflinger, M., et al. (2023). Caspase-8-driven  
1035 apoptotic and pyroptotic crosstalk causes cell death and IL-1 $\beta$  release in X-linked  
1036 inhibitor of apoptosis (XIAP) deficiency. *EMBO J.* 42. 10.15252/embj.2021110468.

1037 75. Wang, Y., and Kanneganti, T.-D. (2021). From pyroptosis, apoptosis and necroptosis

1038 to PANoptosis: A mechanistic compendium of programmed cell death pathways.  
1039 *Comput. Struct. Biotechnol. J.* 19, 4641–4657. 10.1016/j.csbj.2021.07.038.

1040 76. Ponde, N.O., Lortal, L., Tsavou, A., Hepworth, O.W., Wickramasinghe, D.N., Ho, J.,  
1041 Richardson, J.P., Moyes, D.L., Gaffen, S.L., and Naglik, J.R. (2022). Receptor-kinase  
1042 EGFR-MAPK adaptor proteins mediate the epithelial response to *Candida albicans*  
1043 via the cytolytic peptide toxin, candidalysin. *J. Biol. Chem.* 298.  
1044 10.1016/j.jbc.2022.102419.

1045 77. De Nardo, D., Kalvakolanu, D. V., and Latz, E. (2018). Immortalization of Murine Bone  
1046 Marrow-Derived Macrophages. In *Methods in molecular biology* (Clifton, N.J.)  
1047 (Humana Press Inc.), pp. 35–49. 10.1007/978-1-4939-7837-3\_4.

1048 78. Irigoyen, N., Firth, A.E., Jones, J.D., Chung, B.Y.W., Siddell, S.G., and Brierley, I.  
1049 (2016). High-resolution analysis of Coronavirus gene expression by RNA sequencing  
1050 and ribosome profiling. *PLOS Pathog.* 12, e1005473. 10.1371/journal.ppat.1005473.

1051 79. Chung, B.Y.W., Deery, M.J., Groen, A.J., Howard, J., and Baulcombe, D.C. (2017).  
1052 Endogenous miRNA in the green alga *Chlamydomonas* regulates gene expression  
1053 through CDS-targeting. *Nat. Plants* 2017 310 3, 787–794. 10.1038/s41477-017-0024-  
1054 6.

1055 80. Chung, B.Y.W., Balcerowicz, M., Di Antonio, M., Jaeger, K.E., Geng, F., Franaszek,  
1056 K., Marriott, P., Brierley, I., Firth, A.E., and Wigge, P.A. (2020). An RNA thermoswitch  
1057 regulates daytime growth in *Arabidopsis*. *Nat. Plants* 2020 65 6, 522–532.  
1058 10.1038/s41477-020-0633-3.

1059 81. Xiao, Z., Zou, Q., Liu, Y., and Yang, X. (2016). Genome-wide assessment of  
1060 differential translations with ribosome profiling data. *Nat. Commun.* 7.  
1061 10.1038/ncomms11194.

1062 82. Robinson, M.D., McCarthy, D.J., and Smyth, G.K. (2010). *edgeR*: a Bioconductor  
1063 package for differential expression analysis of digital gene expression data.  
1064 *Bioinformatics* 26, 139–140. 10.1093/BIOINFORMATICS/BTP616.

1065 83. Peterson, H., Kolberg, L., Raudvere, U., Kuzmin, I., and Vilo, J. (2020). *gprofiler2* - an  
1066 R package for gene list functional enrichment analysis and namespace conversion  
1067 toolset *g:Profiler*. *F1000Research* 9, 709. 10.12688/f1000research.24956.2.

1068 84. Wise, D. (2019). Understanding antigen processing in chickens using genome editing  
1069 technology. 10.17863/CAM.40666.

1070 85. Amann, E., Ochs, B., and Abel, K.J. (1988). Tightly regulated tac promoter vectors

1071 useful for the expression of unfused and fused proteins in *Escherichia coli*. *Gene* 69,  
1072 301–315. 10.1016/0378-1119(88)90440-4.

1073 86. Bryant, O.J., Dhillon, P., Hughes, C., and Fraser, G.M. (2022). Recognition of discrete  
1074 export signals in early flagellar subunits during bacterial type III secretion. *Elife* 11.  
1075 10.7554/eLife.66264.

1076

**Figure 1**

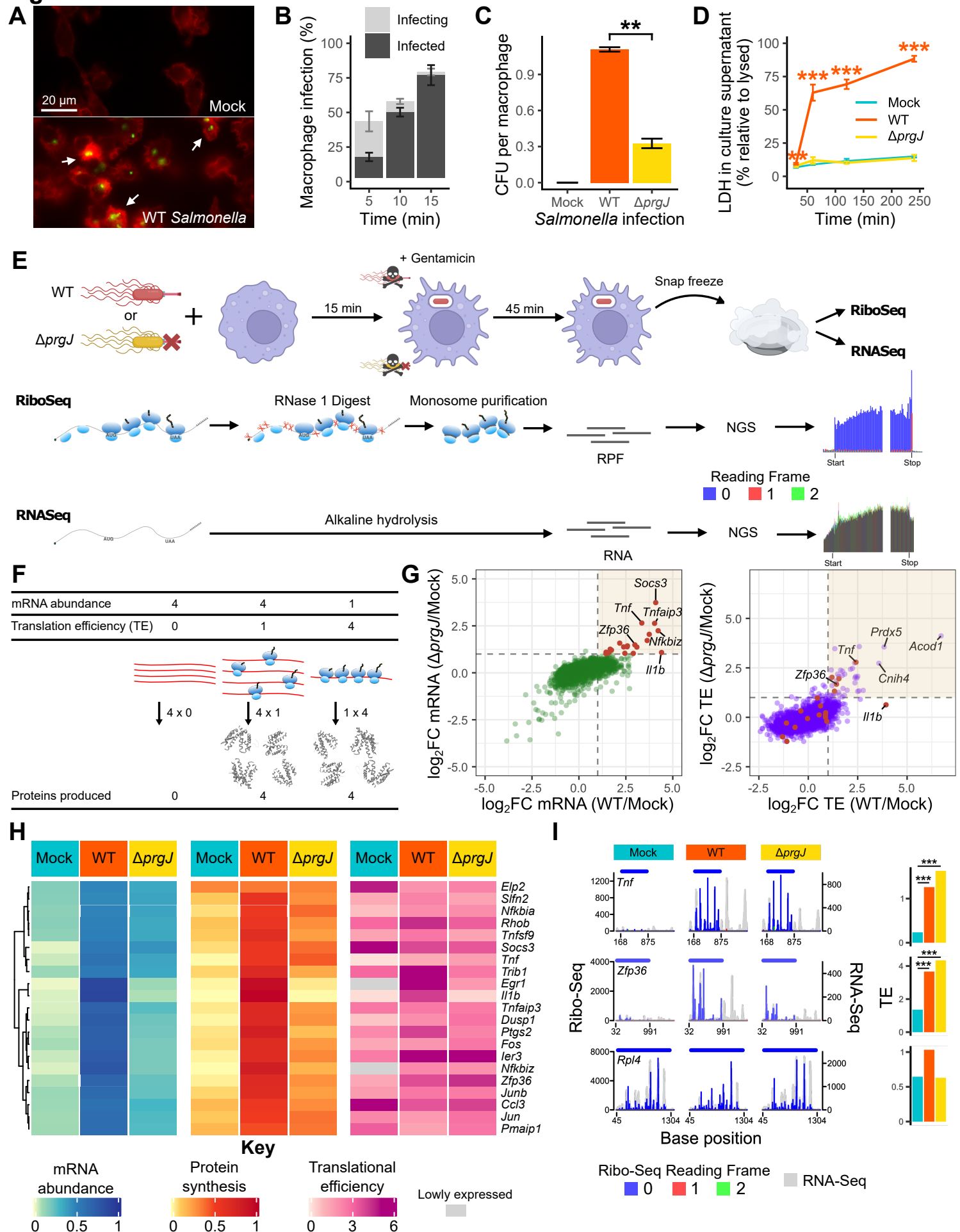


**Figure 1 Cont.**  
**J**

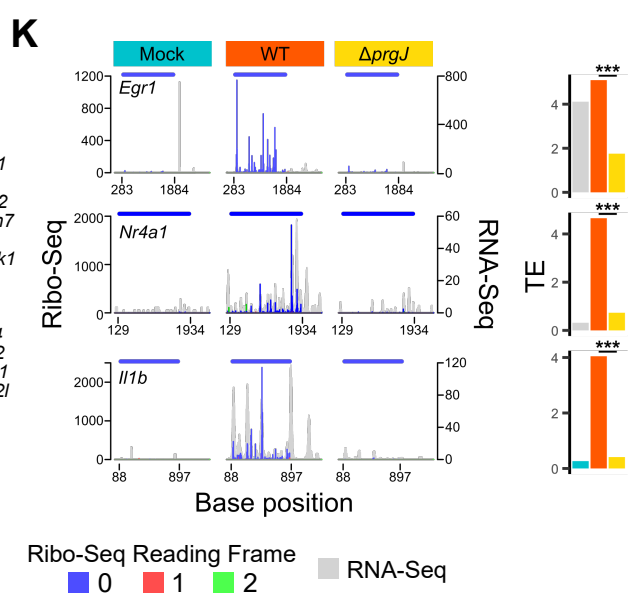
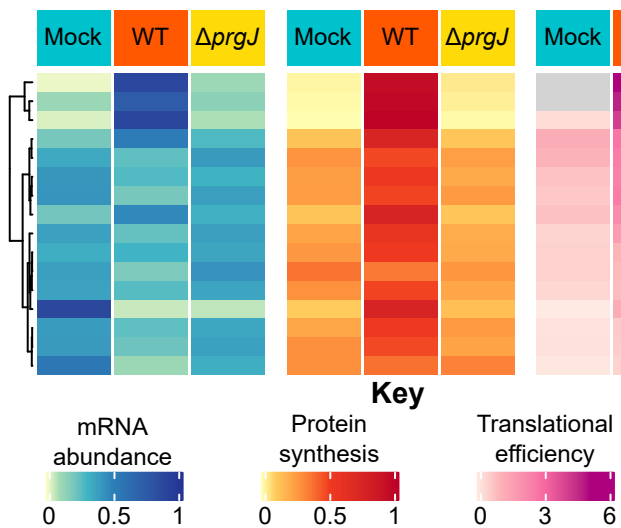


**Figure 2**

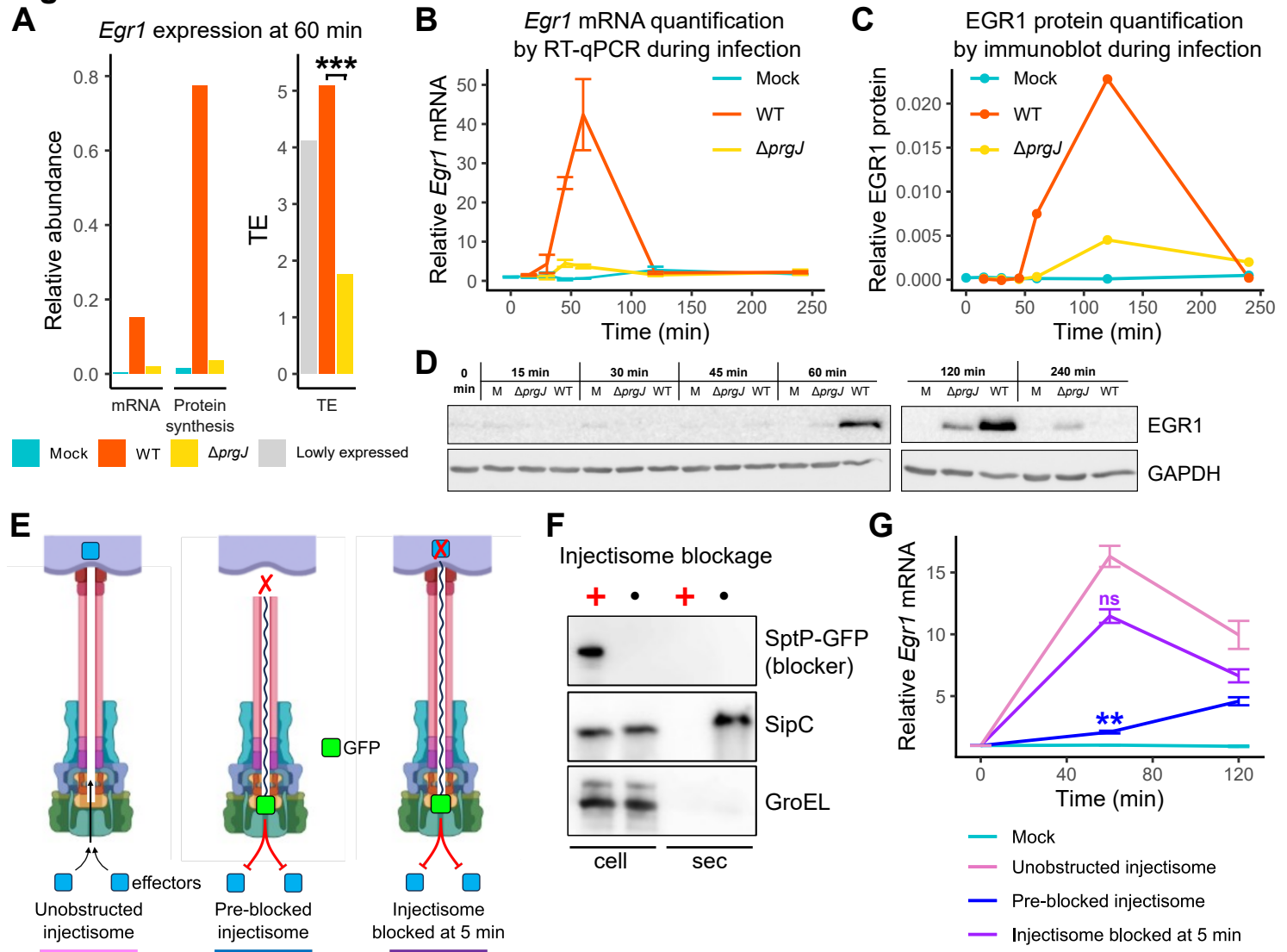
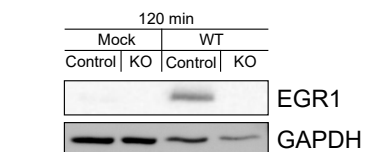
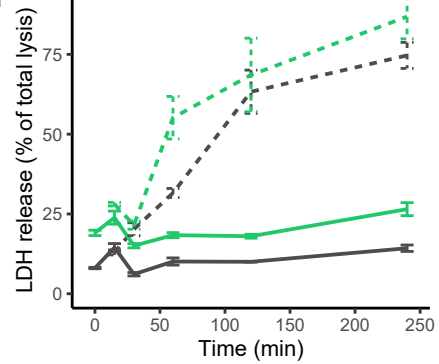


**Figure 2 Cont.**

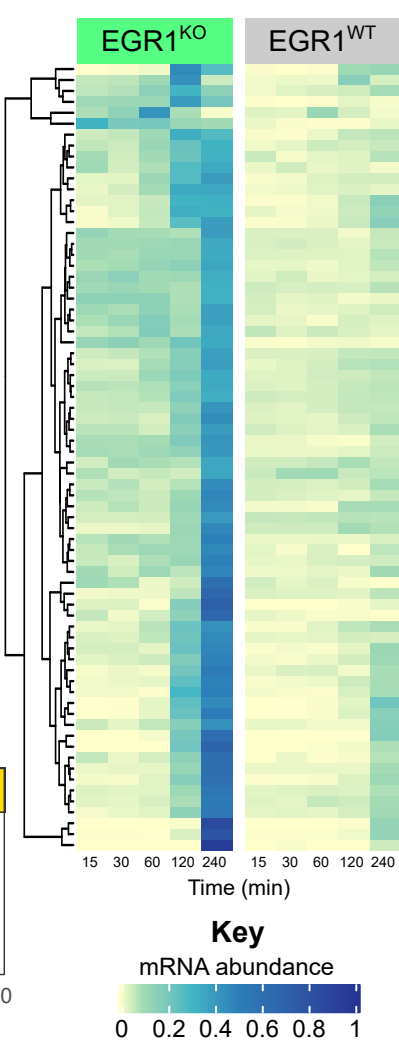
**H**



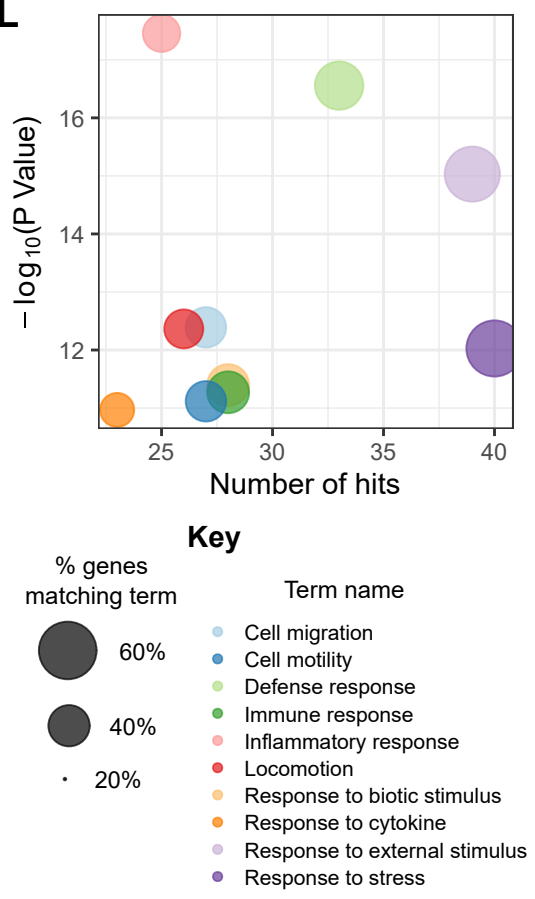
**I**



**K**



**L**



**J**

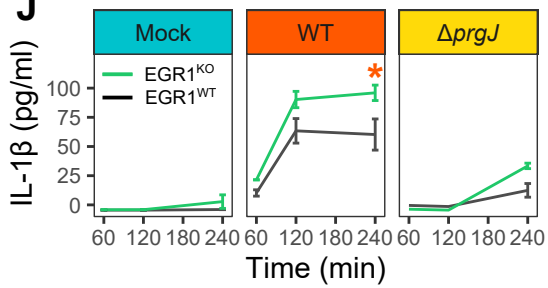
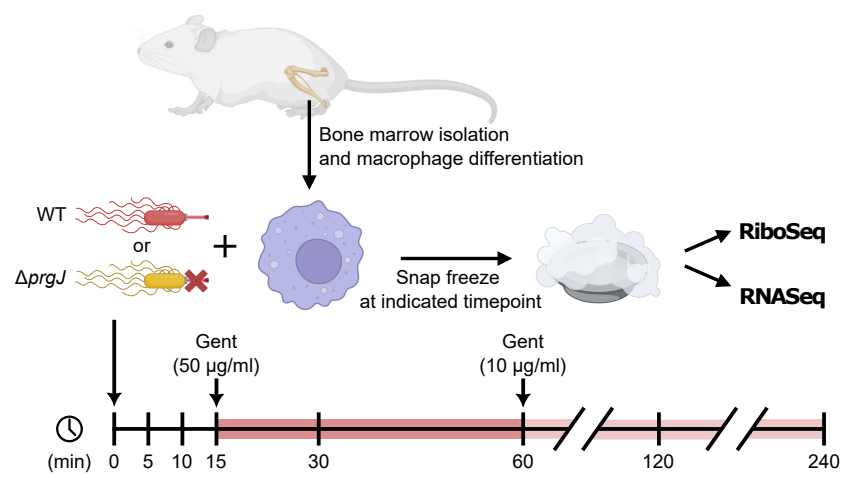


**Figure 3**

**A**



**B**

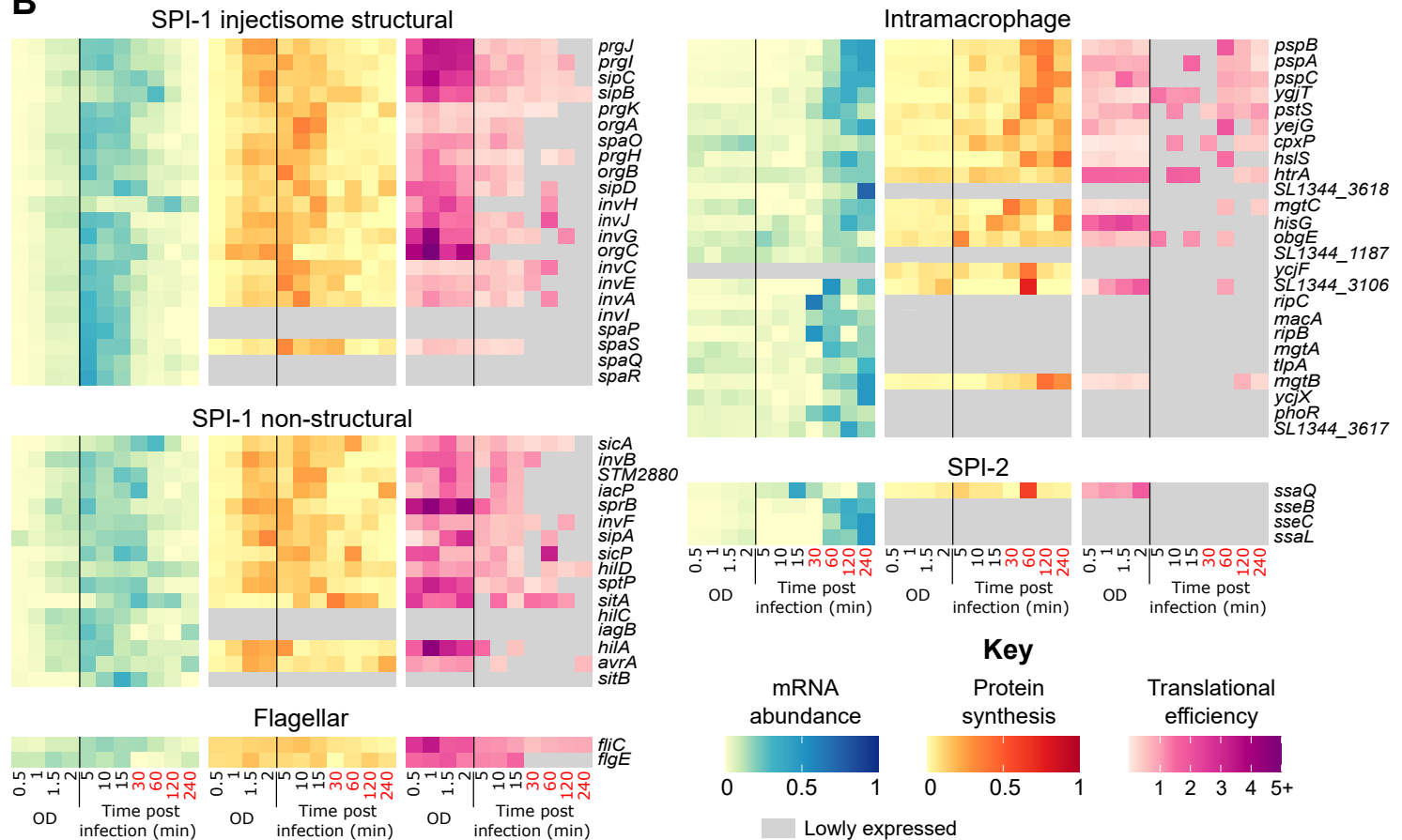
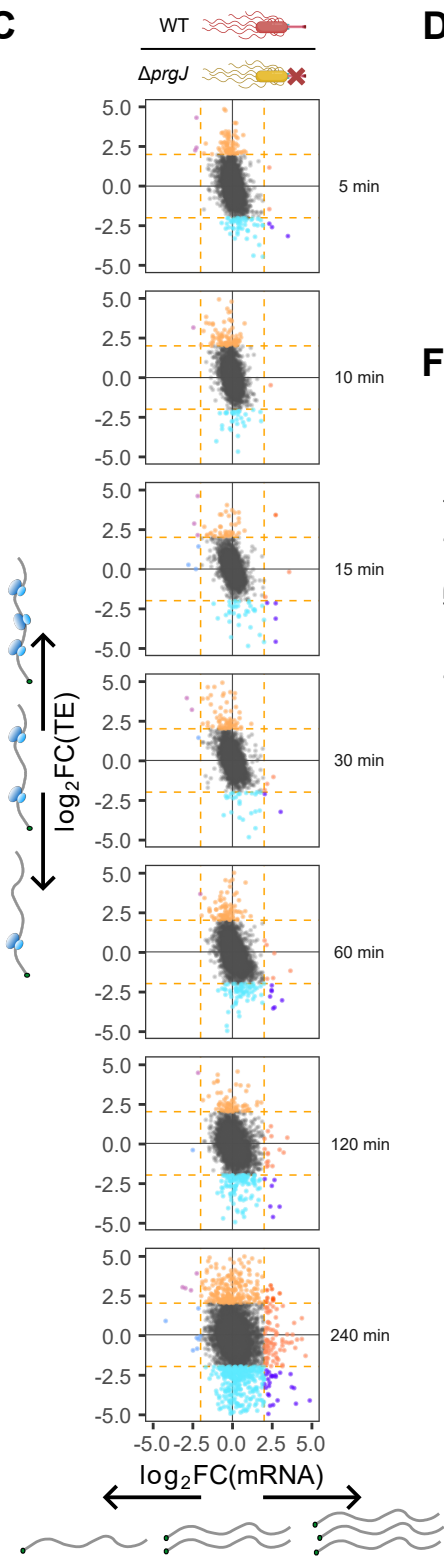
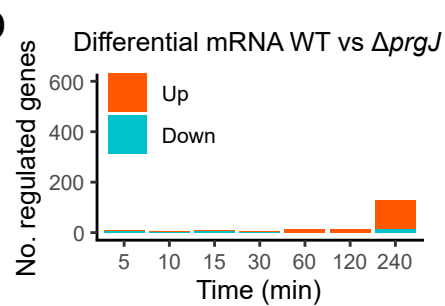


**Figure 3 Cont.**

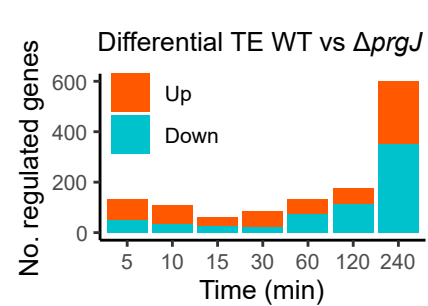
**C**



**D**



**E**



**F**

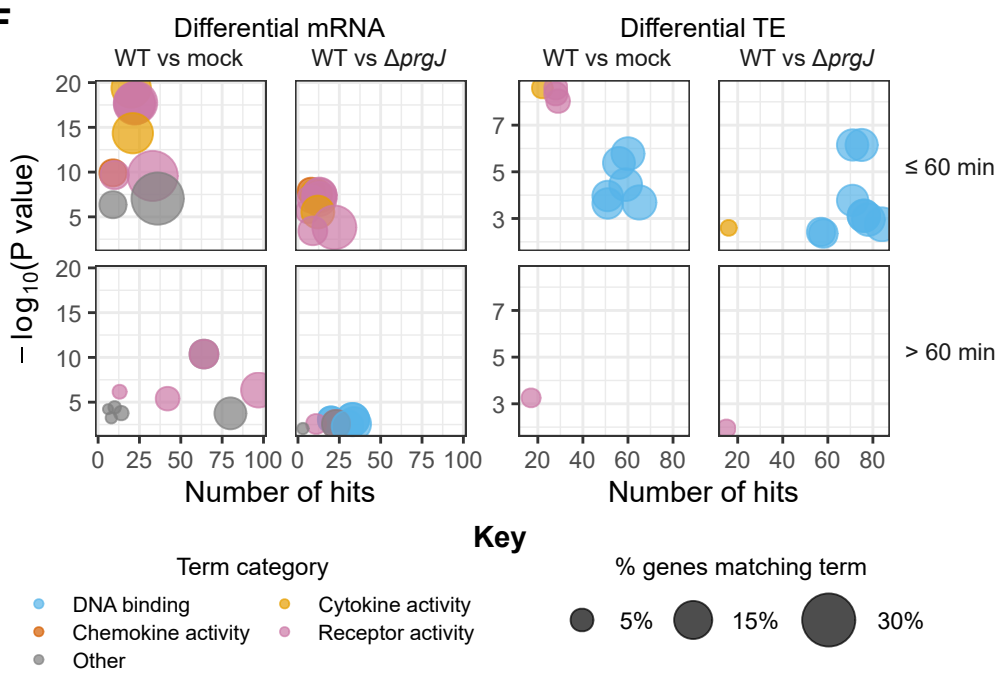


**Figure 4**

